DALTON

Bis[4′-(4-anilino)-2,2′:6′,2″-terpyridine]transition-metal complexes: electrochemically active monomers with a range of magnetic and optical properties for assembly of metallo oligomers and macromolecules†

Gregory D. Storrier, Stephen B. Colbran* and Donald C. Craig

School of Chemistry, University of New South Wales, Sydney, NSW 2052, Australia

The new ligand 4′-(4-anilino)-2,2′:6′,2″-terpyridine (L^1) and a range of its transition-metal complexes have been prepared. The crystal and molecular structures of L^1 and $[CuL^1_2][PF_6]_2$ have been determined. Model reactions show that L^1 and its transition-metal complexes can be functionalised with suitable organic reagents: reactions with aromatic dianhydrides give imide derivatives, reactions with acid chlorides afford amide derivatives and benzoquinone reacts with L^1 to give a quinonylanilinoterpyridine ligand, complexes of which are described, but not with the complexes of L^1. The use of L^1 and its complexes in building up multicomponent architectures has been tested. Metallo-dimers and co-ordination polymers linked by new binucleating bis(terpyridyl) ligands have been prepared by two routes: (*a*) first coupling two L^1 with difunctional organic reagents and then treating the new binucleating ligands with a metal source, or (*b*) preforming monomeric complexes of L^1 and treating these with the same difunctional organic reagents. Analytical, spectroscopic and electrochemical data are given for all complexes; the chromophoric, magnetic and electrochemical properties of the complexes vary with transition metal and terpyridyl ligand substituent.

Aromatic tetracarboxylic dianhydrides and aromatic diamines co-condense to give polyimides which exhibit desirable physical properties such as regular, well characterised rigid-rod structures and outstanding thermal stabilities.[1] A recent and important objective has been the incorporation of polyimides and other polymer systems with dye-containing pendant groups, research spurred on by the expectation that materials will be obtained with excellent properties for use in optical devices.[1–3] There is a parallel and burgeoning interest in macromolecules incorporating transition metals; as well as desirable optical properties, these materials offer unusual and potentially useful magnetic or electrical properties.[3–5]

Bis(terpyridyl) transition-metal complexes[6] are simply prepared, more often than not are stable in more than one accessible oxidation state, and offer a wide spectrum of magnetic,[7] photophysical[8] and electrochemical properties.[9,10] It is therefore no surprise that they have found much recent use as the electroactive and chromophoric centres in supramolecular assemblies.[5,10–12] Other recent studies of photoinduced charge separation in porphyrin–diimide assemblies and porphyrin–diimide–quinone triads and tetrads show that the diimide centres not only act as rigid spacers but also that they are redox active and take part in the initial charge-separation process by acting as electron acceptors to the singlet excited state of the porphyrins.[13] Taken together the above results suggest that rigid-rod polymers formed from alternating bis(terpyridyl) transition metal and diimide centres will have novel optical, magnetic and/or electrical properties. Recent reports of the novel photorefractive behaviour exhibited by polyimide polymers with porphyrin centres interspersed throughout the polymer chain[3] add further weight to this prediction and prompts us to report: (*i*) the syntheses and properties of new redox-active and chromophoric monomers of the general formula $[ML^1_2]^{n+}$ where M is a transition metal and L^1 is the new ligand 4′-(4-anilino)-2,2′:6′,2″-terpyridine; (*ii*) model reactions of $[FeL^1_2]^{2+}$ and $[Ru(terpy)L^1]^{2+}$ (terpy = 2,2′:6′,2″-terpyridine) with monofunctional organic reagents demonstrating that these two complexes, and by inference all the complexes, undergo polymerisation reactions typical of aromatic diamines;[1–3,14] and (*iii*) results showing that oligomers and polymers are available from L^1 and its transition-metal complexes. Some of these results have appeared in a preliminary communication.[15]

† *Non-SI units employed*: $\mu_B \approx 9.27 \times 10^{-24}$ J T^{-1}, mmHg ≈ 133 Pa.

Results and Discussion

Synthetic studies

Synthesis of L^1. Given the recent interest in transition-metal complexes of terpyridines with 4′-pendants,[5–12] it is surprising that the ligand L^1 has not been reported. However, we find that L^1 can be obtained by two methods (see Scheme 1): a conventional one-pot condensation of poly(4-aminobenzaldehyde) and 2 equivalents of 2-acetylpyridine or a two-step terpyridine synthesis[6,16] starting from 4-aminobenzaldehyde and two equivalents of 2-acetylpyridine; here the 4-aminobenzaldehyde[17] was prepared immediately prior to the ligand preparation and was handled in caustic-treated glassware (to prevent its acid-catalysed self-condensation). In our hands, the two-step synthesis was poorly reproducible and the reliable one-pot condensation of poly(4-aminobenzaldehyde), which, conveniently, is commercially available, and 2-acetylpyridine is preferred.

Monomeric complexes of L^1. Reactions of 2 equivalents of L^1 with the appropriate metal chloride salt in methanol heated at reflux for ≈15 min produced the complex cations $[ML^1_2]^{2+}$ (M = Mn, Co, Ni, Cu or Zn), which were most conveniently isolated as their hexafluorophosphate salts in 75–90% yield after metathesis with saturated methanolic $[NH_4][PF_6]$ and recrystallisation from methanol. Reaction of $RhCl_3 \cdot 3H_2O$ with 2 equivalents of L^1 in boiling methanol followed by metathesis with aqueous $[NH_4][PF_6]$ afforded $[RhL^1_2][PF_6]_3$ in 62% yield, $[FeL^1_2]^{2+}$ was obtained in 80% yield as its tetrafluoroborate salt directly from the reaction of $[Fe(H_2O)_6][BF_4]_2$ with 2 equivalents of L^1 in methanol, and $[RuL^1_2][PF_6]_2$ was obtained in 55% yield from the reaction of L^1 and $[RuCl_2(dmso)_4]$ (dmso = dimethyl sulfoxide) in aqueous ethanol heated at reflux for 3 h, followed by metathesis with methanolic $[NH_4][PF_6]$. Reduction of $[Ru(terpy)Cl_3]$ with triethylamine in the presence of L^1 in hot

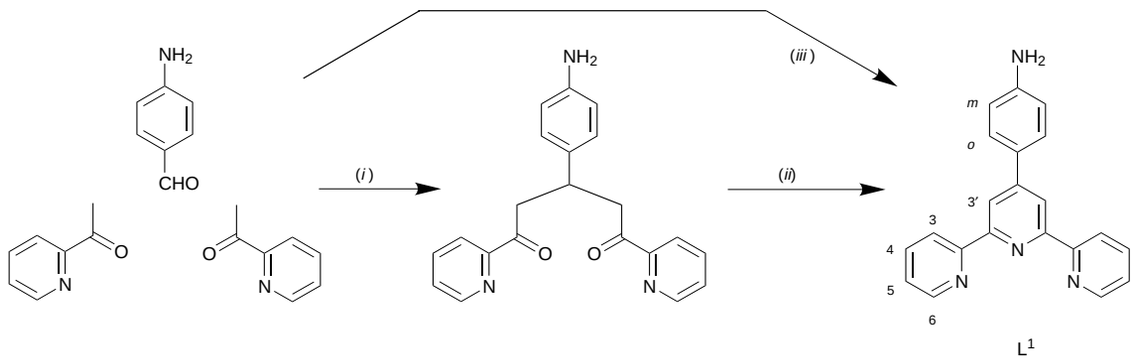

Scheme 1 (*i*) NaOH (aq), EtOH, 24 h; (*ii*) $[NH_4][O_2CMe]$, EtOH, heat, 4 h, yield 14% overall for steps (*i*) and (*ii*); (*iii*) $[NH_4][O_2CMe]$, acetamide, heat, 2 h; NaOH (aq), heat 2 h; $MeCO_2H$, 48% HBr (aq); $NaHCO_3$, $CHCl_3$, yield 12%

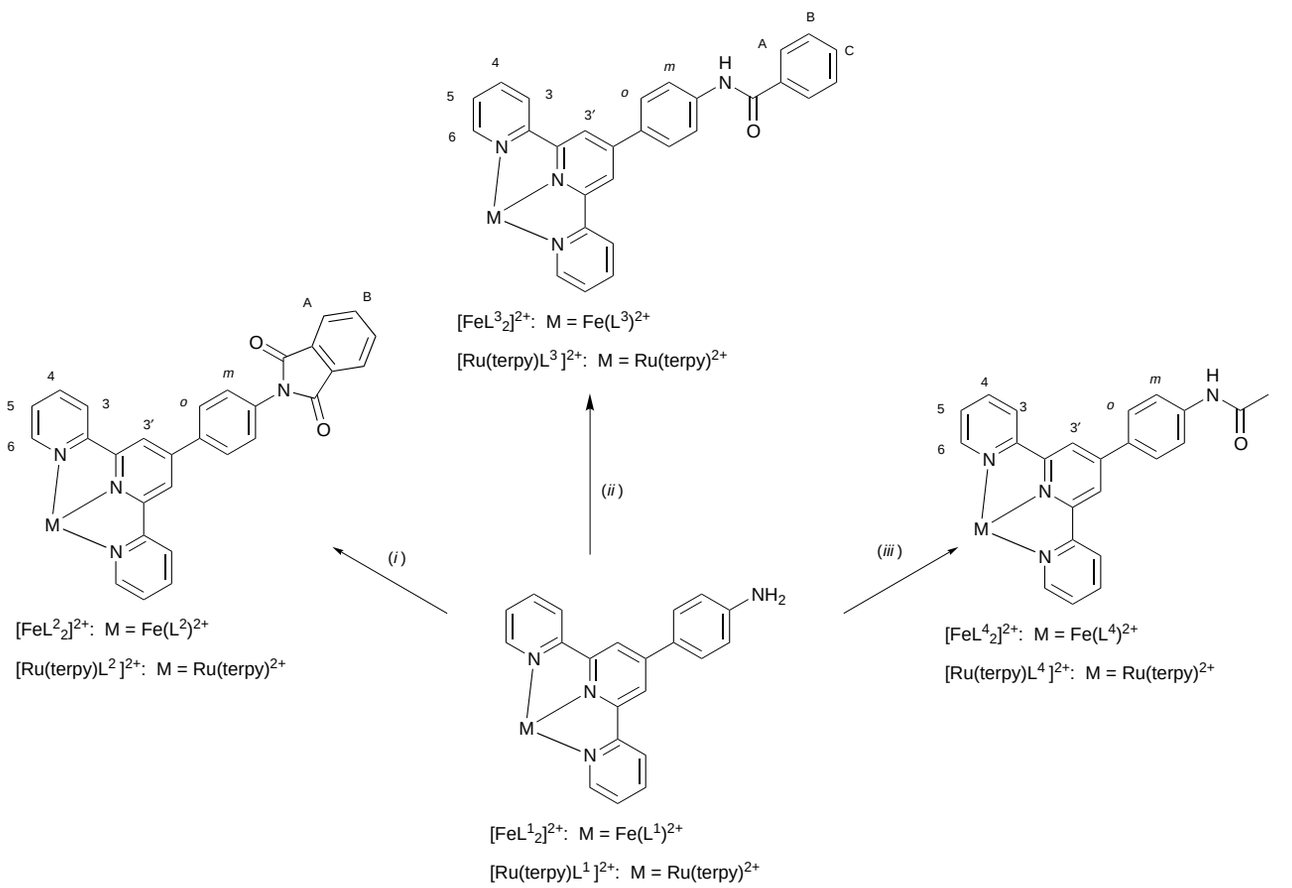

Scheme 2 (*i*) Phthalic anhydride in dimethylacetamide followed by pyridine–acetic anhydride at 80 °C, or phthalic anhydride in *N*-methylpyrrolidinone, 120 °C, 20 h; (*ii*) benzoyl chloride in acetonitrile–pyridine, heat; (*iii*) acetyl chloride in acetonitrile–pyridine, heat

aqueous ethanol, followed by addition of saturated aqueous $[NH_4][PF_6]$, afforded $[Ru(terpy)L^1][PF_6]_2$ in 55% yield.

Model oligomerisation/polymerisation reactions. There are two general routes to oligomers or polymers derived from L^1 and its transition-metal complexes: either (*a*) first preparing a multinucleating terpyridyl ligand by coupling two or more L^1 together with a multifunctional organic reagent followed by addition of metal ions to form the co-ordination oligomer or polymer, or (*b*) linking preformed monomeric complexes of L^1, *e.g.* $[ML^1_2]^{n+}$ (M = transition-metal ion), with the same multifunctional reagent. Most successful syntheses of oligomers linked by multinucleating terpyridyl ligands have been prepared by preforming the ligand [route (*a*)], although Constable and co-workers[11a–d] have recently reported some ether-linked bis(terpyridyl)ruthenium oligomers prepared by route (*b*).

Two classes of polymer commonly formed from aromatic diamines are polyimides [from condensation with bis(acid dianhydrides), *e.g.* pyromellitic dianhydride (benzene-1,2:4,5-tetracarboxylic dianhydride)] and polyamides [from condensation with bis(acid chlorides), *e.g.* terephthaloyl chloride].[1,2,14] To investigate the feasibility of using L^1 and its transition-metal complexes in analogous oligomerisation or polymerisation reactions, model reactions were carried out on L^1 itself and on $[FeL^1_2]^{2+}$ and $[Ru(terpy)L^1]^{2+}$. As expected, simple condensations of L^1 with phthalic anhydride or with benzoyl chloride gave high yields (>90% raw yield; 65–70% isolated yield) of the phthalimidophenyl and benzamidophenyl substituted ligands, L^2 and L^3 respectively (see Scheme 2 for the ligand nomenclature adopted). Next the reactions of $[FeL^1_2]^{2+}$ and $[Ru(terpy)L^1]^{2+}$ were investigated in order to establish whether or not the reactivity of the anilino-function would be diminished by co-ordination to the electrophilic metal centres. The reactions attempted, conditions used and the nomenclature adopted for the complexes of the new ligands are summarised in Scheme 2. The raw yields of the imide complexes, $[FeL^2_2]^{2+}$ and $[Ru(terpy)L^2]^{2+}$, and the amide complexes, $[FeL_2]^{2+}$ and $[Ru(terpy)L]^{2+}$ (L = L^3 or L^4), ascertained by ^{1}H NMR spec-

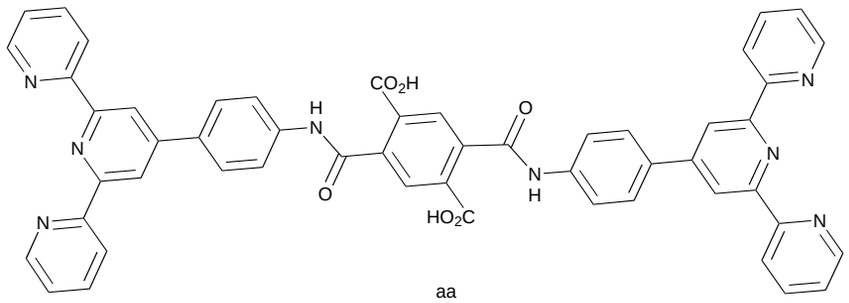

aa

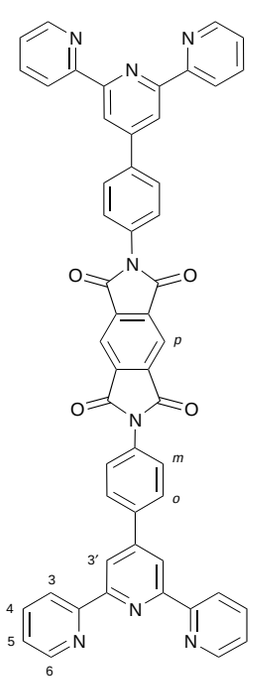

L^5

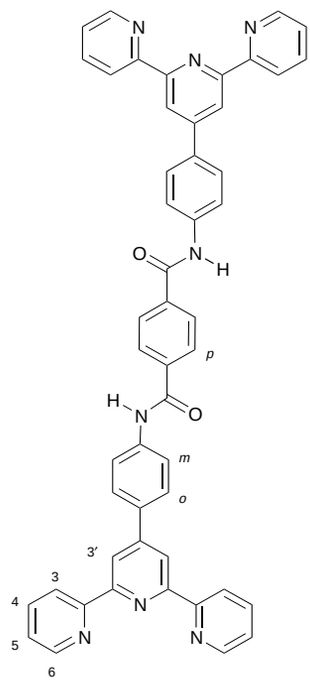

L^6

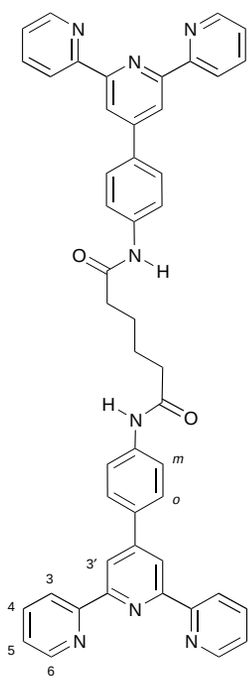

L^7

troscopy (the solvent was stripped from the reaction mixture, the resulting solid redissolved in deuteriated solvent and the ^{1}H NMR spectrum run), were high (90% and better). However, isolated yields of these products dropped to around 50–60% following purification by flash chromatography (silica support; eluent acetonitrile–water–saturated aqueous KNO_3 20:2:1) and recrystallisation from a solution of an excess of $[NH_4][PF_6]$ in aqueous acetonitrile. If the chromatography step was omitted and the crude solid obtained on removing the solvent from the reaction mixture was recrystallised, much higher yields (typically 70–85%) of equally pure product were obtained.

These results suggest that L^1 and its complexes can be functionalised in high yield but that losses occur during purification of the crude product, and that chromatography needs to be avoided if high yields are to be obtained. With this in mind, studies of oligomer and polymer formation were begun.

Preliminary studies of oligomer and polymer formation. To demonstrate both routes, (*a*) treating a preformed multinucleating terpyridyl ligand with a metal source and (*b*) linking preformed transition-metal complexes of L^1, in construction of supramolecular architectures, we investigated the preparations of three binuclear ruthenium(II) complexes, [(terpy)Ru(L–L)-Ru(terpy)]$^{4+}$ (L–L = L^5–L^7). First, route (*a*), preforming the binucleating bis(terpyridyl) ligands. Reaction of two equivalents of L^1 with pyromellitic dianhydride in 1-methylpyrrolidin-2-one (nmp) at room temperature followed by addition of acetic anhydride and pyridine and heating to 80 °C [14] to close the intermediate amic acid (aa) produced L^5 in 91% isolated yield. Diamidoaryl-bridged L^6 was obtained in 70% isolated yield from 2 equivalents of L^1 with terephthaloyl chloride in dimethylacetamide (dma)–pyridine (4:1) solution, and diamidoalkyl-bridged L^7 was obtained in 73% yield from 2 equivalents of L^1 with adipoyl chloride in hot (120 °C) dma–pyridine (4:1) solution. The new binucleating ligands, L^5–L^7, were only sparingly soluble in high-boiling, polar aprotic solvents, and in anhydrous trifluoroacetic acid. Nevertheless, suspensions of them in boiling dimethylformamide (dmf) or boiling ethane-1,2-diol dissolved when treated with 2 equivalents of $[Ru(terpy)(Me_2CO)_3]^{3+}$ {generated from $[Ru(terpy)Cl_3]$ and 3 equivalents of $AgSbF_6$ in dry acetone} or with $[Ru(terpy)Cl_3]$ respectively. Each of these reactions produced a mixture of complexes which was separated by flash chromatography (silica support; eluent MeCN–water–saturated aqueous KNO_3 20:2:1), with the first band eluted yielding $[Ru(terpy)_2]^{2+}$ (8–20%), the second impure $[Ru(terpy)(L–L)]^{2+}$ (L–L = L^5–L^7) and the third [(terpy)Ru(L–L)Ru(terpy)]$^{4+}$ (L–L = L^5–L^7) (32–48%).

Secondly, route (*b*), linking preformed complexes of L^1. The dimer [(terpy)RuL^5Ru(terpy)]$^{4+}$ was also obtained from $[Ru(terpy)L^1]^{2+}$ and pyromellitic dianhydride in dma at reflux, followed by pyridine–acetic anhydride (1:2) to effect cyclodehydration in 40% yield. The amido-bridged dimers, [(terpy)Ru(L–L)Ru(terpy)]$^{4+}$ (L–L = L^6 or L^7), were also obtained from $[Ru(terpy)L^1]^{2+}$ and either terephthaloyl chloride in dma–pyridine at reflux or adipoyl chloride in dmf–pyridine at reflux in 44 and 30% yields respectively. Again, $[Ru(terpy)_2]^{2+}$ was a product in these reactions.

That $[Ru(terpy)_2]^{2+}$ was always a product in the above reac-

tions [for both routes (*a*) and (*b*)] indicates redistribution of the terpyridyl ligands between metal centres occurs under the forcing reaction conditions,[12] and this and the chromatography necessary to separate these products combine to reduce the overall yield of pure targeted dimer. In syntheses of higher mixed-ligand oligomers, such processes will be exacerbated leading to still lower yields. However, polymerisations using either route (*a*) or (*b*) to form the homopolymers $[\{M(L{-}L)\}_n]^{2n+}$ [L–L = binucleating bis(terpyridyl) ligand] should avoid the problems associated with ligand-scrambling reactions and are described next.

We investigated the preparations of the iron(II) homopolymers, $[\{Fe(L{-}L)\}_n]^{2n+}$ (L–L = L^5–L^7). Route (*b*): $[FeL^1{}_2][BF_4]_2$ was coupled either with stoichiometric pyromellitic dianhydride in dma at reflux, followed by pyridine–acetic anhydride (1 : 2) to effect cyclodehydration[14] to give crude $[(FeL^5)_n][BF_4]_{2n}$, or with terephthaloyl chloride or adipoyl chloride in dma–pyridine at reflux to give crude $[(FeL^6)_n][BF_4]_{2n}$ or $[(FeL^7)_n][BF_4]_{2n}$ respectively. Exhaustive extraction with methanol and with acetone to remove lower-molecular-weight oligomers, followed by fractional precipitation from dmf–CH_2Cl_2, afforded $[(FeL^5)_n][BF_4]_{2n}$ in 83% yield, $[(FeL^6)_n][BF_4]_{2n}$ in 60% yield and $[(FeL^7)_n][BF_4]_{2n}$ in 52% yield. Route (*a*): a sample of $[(FeL^5)_n][BF_4]_{2n}$ was also obtained by treating the binucleating bis(terpyridyl) ligand L^5 with equimolar $[Fe(H_2O)_6][BF_4]_2$ in boiling dma. This sample was purified as above and displayed the same electronic and NMR spectra (see below) as the material obtained by route (*b*). The three co-ordination polymers were soluble in warm high-boiling, polar, aprotic solvents such as dma, dmf, nmp and dimethyl sulfoxide, and in anhydrous trifluoroacetic acid.

Attempted formation of poly(quinonylanilinoterpyridine)-transition-metal oligomers and polymers. Polyquinonylamines are an interesting group of redox-active polymers having potential as anticorrosion agents with the ability to displace water from, for example, wet, rusty iron surfaces.[18] These polymers are formed in straightforward condensations (successive Michael addition and oxidation reactions) of benzoquinone with diamines. The success of the preliminary studies of oligomer and polymer formation described above suggested that poly(quinonylanilinoterpyridine)transition-metal complexes should also be available by two routes: (*a*) preforming the new dinucleating terpyridyl ligand L^8 by treating L^1 with benzoquinone and then with appropriate metal sources, and (*b*) from condensations of $[ML^1{}_2]^{2+}$ monomers with benzoquinone. The attraction of co-ordination oligomers or polymers of L^8 lies in the fact that the quinonyl bridging group will be redox active and potentially could act as an electron acceptor in systems with photoactive bis(terpyridyl)-ruthenium or -osmium centres.

Unfortunately complexes of L^8 were not available by either route. Route (*b*): the complexes $[FeL^1{}_2]^{2+}$ and $[Ru(terpy)L^1]^{2+}$ were treated with benzoquinone under a variety of conditions, for example heating at reflux in ethanol, always with the same result, no reaction between the complexes and benzoquinone was observed. We conclude that the nucleophilicity of the anilino group(s) in the complex dications is reduced to the point where Michael addition to benzoquinone does not occur. Next, route (*a*), preforming L^8. The literature procedure for the formation of 2,5-dianilino-1,4-benzoquinone involves reaction of stoichiometric quantities of benzoquinone and aniline in ethanol heated at reflux.[18,19] Using this procedure, equimolar amounts of L^1 and 1,4-benzoquinone afforded a dark red solid in 34% yield following recrystallisation from ethanol which was identified (see below) as the quinonylanilinoterpyridine ligand, L^9. Reactions of an excess of L^1 with benzoquinone were also tried and afforded L^9 but none of the targeted binucleating ligand, L^8. As well, no reaction occurred between L^1 and benzoquinone in tetrahydrofuran or in acetic acid–water–ethanol mixtures. Some complexes of L^9 were prepared. The homoleptic complexes $[ML^9{}_2]^{2+}$ (M = Fe, Co or Zn) were

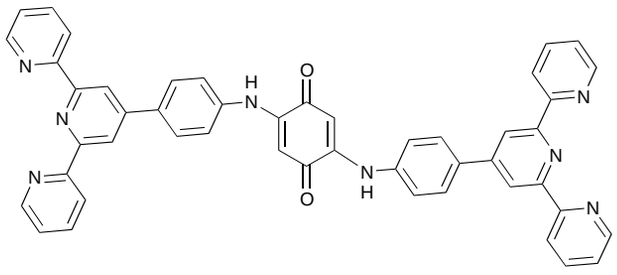

L^8

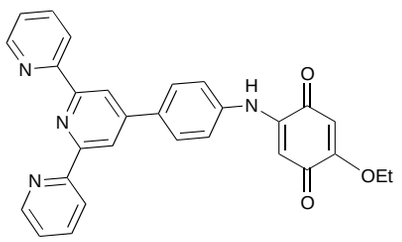

L^9

obtained from reactions of L^9 with $CoCl_2{\cdot}6H_2O$, $[Fe(H_2O)_6][BF_4]_2$ and $Zn(O_2CMe)_2$ respectively, and reaction of $[Ru(terpy)Cl_3]$ with L^9 in refluxing ethanol–water solution afforded $[Ru(terpy)L^9]^{2+}$. Final yields of the complexes after chromatography and recrystallisation were 45–65%.

Characterisation and properties of the new compounds

Ligands. Only ligands L^1–L^3, L^5–L^7 and L^9 were isolated. The analytical and spectroscopic data for L^1, isolated as stable, pale yellow microcrystals (m.p. 256–257 °C), are fully in accord with its formulation. It exhibited a broad amine N–H stretch at 3330 cm^{-1} in its IR spectrum and a molecular ion at *m*/*z* 324 in its electron impact (EI) mass spectrum. The ^1H NMR spectrum of L^1 shows peaks for each set of magnetically inequivalent protons (five pyridyl, two phenyl and the amine protons) and a ^{13}C-{^1H} NMR spectrum reveals the expected 12 peaks. Likewise the analytical and spectroscopic data are consistent for L^2, L^3, L^5–L^7 and L^9. For example, the imide C=O band was found at 1740 cm^{-1} in the IR spectrum of L^5, amide C=O peaks for L^6 and L^7 are observed at 1670 and 1655 cm^{-1} respectively, and L^9 shows a strong quinonyl C=O band at 1665 cm^{-1}. The EI mass spectra showed strong peaks for the expected molecular ions and the ^1H and ^{13}C-{^1H} NMR spectra revealed peaks for the requisite number of magnetically inequivalent protons or carbon atoms, respectively, for the structures given for each ligand. Absorption spectra of the ligands (Table 1) reveal a collection of $\pi \longrightarrow \pi^*$ or $n \longrightarrow \pi^*$ bands (below ≈410 nm) which tail into the visible region. The intense band at 497 nm in the electronic spectrum of L^9 in methanol accounts for the red colour of this ligand and is very likely centred on the anilinoquinone group (for comparison, 2-anilino-1,4-benzoquinone in dmf shows an intense band at 497 nm[19]). The UV/VIS spectrum of L^1 is given in Fig. 1 along with examples of spectra of imide (L^2) and amide (L^3) derivatives.

Crystal structure of L^1. The ligand L^1 crystallised from chloroform–methanol solution in the space group $P2_1/c$ with eight molecules in the unit cell. There are two independent molecules of L^1, L^1(A) and L^1(B), in the crystal structure. Selected bond length and angle data are listed in Table 2. Fig. 2 presents a view of the crystal structure of L^1 (down the *c* axis). The crystal structure consists of oblique columns running parallel to the *a* axis formed by offset π stacking between the terpyridyl groups in anilino-tail-to-anilino-tail pairs of L^1(A) alternating with anilino-tail-to-anilino-tail pairs of L^1(B). The parallel molecules within each of the tail-to-tail pairs of L^1(A) and tail-

Table 1 Electronic spectral data for the ligands and complexes

Compound	λ_{max}/nm (10^{-3} ε/l mol^{-1} cm^{-1})
L^1 [a]	408 (11.3), 326 (16.8), 314 (15.8), 286 (24.4), 234 (22.2), 204 (35.5)
L^2 [a]	285 (38.5), 228 (36.9), 209 (38.2)
L^3 [b]	309 (sh, 18.9), 286 (20.6), 229 (19.5)
L^5 [b]	286 (12.5)
L^6 [b]	321 (34.6), 297 (sh, 34.4), 287 (35.3)
L^7 [b]	297 (36.7)
L^9 [b]	497 (3.8), 310 (sh, 21.8), 285 (30.7), 231 (24.9), 209 (31.4)
$[CoL^1_2][PF_6]_2$ [a]	716 (sh, 0.20), 411 (53.9), 312 (66.3), 284 (84.6), 205 (141.6)
$[CuL^1_2][PF_6]_2$ [a]	685 (0.10), 414 (46.8), 286 (44.2), 234 (37.6), 232 (63.6), 204 (90.1)
$[MnL^1_2][PF_6]_2$ [a]	404 (61.1), 325 (67.7), 315 (63.7), 286 (95.8), 235 (91.9), 204 (140.5)
$[NiL^1_2][PF_6]_2$ [a]	804 (0.13), 409 (54.3), 327 (32.5), 314 (34.9), 279 (53.5), 236 (45.0), 205 (92.2)
$[RhL^1_2][PF_6]_2$ [a]	480 (43.4), 347 (24.0), 331 (32.0), 298 (52.8), 288 (52.0), 247 (42.8)
$[RuL^1_2][PF_6]_2$ [a]	507 (44.1), 308 (97.7), 285 (57.6), 276 (53.1), 235 (46.1)
$[ZnL^1_2][PF_6]_2$ [a]	407 (46.9), 326 (44.5), 315 (40.4), 285 (59.6), 235 (61.0), 206 (84.2)
$[FeL^1_2][BF_4]_2$ [a]	577 (30.2), 378 (26.9), 320 (51.3), 285 (47.7), 277 (39.7), 233 (sh, 35.8)
$[FeL^2_2][BF_4]_2$ [a]	574 (22.7), 322 (46.7), 285 (41.9), 278 (34.1)
$[FeL^3_2][BF_4]_2$ [a]	571 (34.1), 326 (77.2), 285 (62.7), 277 (50.5), 205 (109.5)
$[FeL^4_2][BF_4]_2$ [a]	571 (27.4), 323 (62.0), 284 (51.7), 277 (42.0), 225 (sh, 45.0)
$[Ru(terpy)L^1][PF_6]_2$ [a]	491 (33.0), 309 (94.0), 273 (51.2), 203 (84.1)
$[Ru(terpy)L^2][PF_6]_2$ [a]	485 (25.8), 308 (76.6), 283 (41.8), 273 (44.7), 229 (sh, 40.2)
$[Ru(terpy)L^3][PF_6]_2$ [a]	485 (32.3), 309 (95.8), 282 (56.2), 273 (60.2), 225 (sh, 58.0)
$[Ru(terpy)L^4][PF_6]_2$ [a]	485 (25.9), 308 (78.3), 282 (49.5), 273 (53.5), 227 (sh, 42.6)
$[(terpy)RuL^5Ru(terpy)][PF_6]_4$ [c]	484 (46.9), 308 (151.5), 286 (sh, 102.5), 275 (98.1), 220 (105.1)
$[(terpy)RuL^6Ru(terpy)][PF_6]_4$ [c]	485 (47.4), 327 (sh, 95.6), 309 (130.4), 280 (sh, 69.7), 272 (77.3), 230 (sh, 75.0)
$[(terpy)RuL^7Ru(terpy)][PF_6]_4$ [c]	485 (41.3), 330 (sh, 79.0), 308 (126.8), 281 (79.9), 273 (86.3), 230 (sh, 69.0)
$[(FeL^5)_n][BF_4]_{2n}$ [b]	578, 326, 289
$[(FeL^6)_n][BF_4]_{2n}$ [b]	578, 325, 288
$[(FeL^7)_n][BF_4]_{2n}$ [b]	577, 317, 288
$[CoL^9_2][PF_6]_2$ [c]	490 (17.5), 323 (53.9), 283 (70.5), 276 (sh, 65.9), 210 (91.6)
$[FeL^9_2][BF_4]_2$ [c]	577 (36.1), 350 (sh, 55.0), 321 (57.2), 284 (66.6), 277 (58.8), 220 (sh, 51.3)
$[ZnL^9_2][PF_6]_2$ [c]	492 (13.7), 337 (sh, 59.4), 327 (61.3), 284 (77.1), 237 (65.4), 210 (88.2)
$[Ru(terpy)L^9][PF_6]_2$ [c]	489 (25.5), 308 (69.5), 281 (46.1), 273 (50.0), 239 (sh, 33.7), 208 (59.8)

[a] In methanol. [b] In dmf. [c] In acetonitrile.

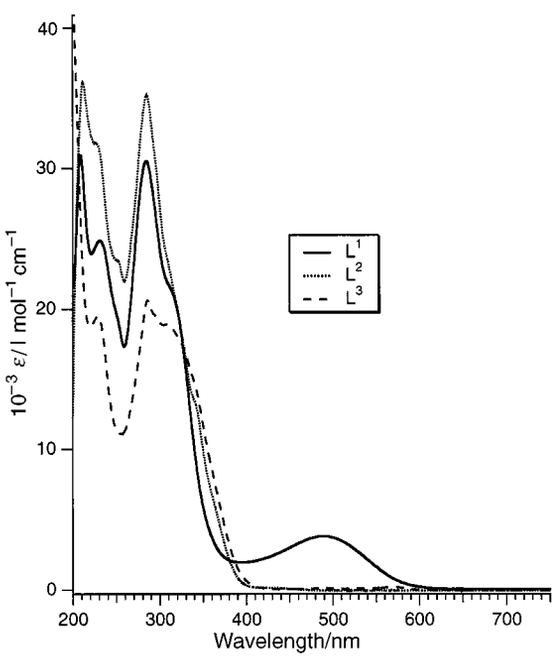

Fig. 1 The UV/VIS spectra of compounds L^1–L^3 in methanol

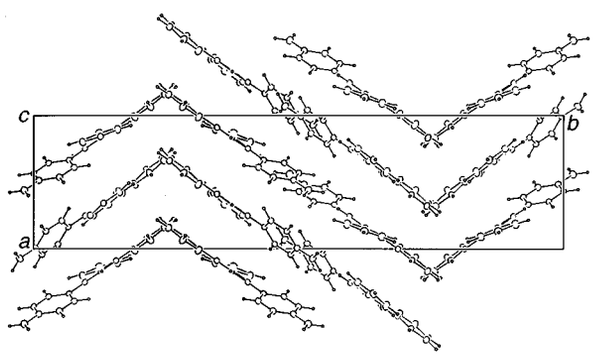

Fig. 2 Packing of the molecules in the crystal structure of compound L^1, viewed down the *c* axis

to-tail pairs of L^1(B), which form the oblique plates that stack to form each column, are related by crystallographic inversion.The distance between the π-stacked terpyridyl groups is 3.5 Å. The molecules of L^1 in adjacent columns are arranged in an offset herringbone structure with respect to each other.

Both independent molecules of L^1 display similar metrical parameters. The molecular structure of L^1(A) is shown in Fig. 3. In L^1(A) and L^1(B) the three pyridyl rings are approximately coplanar and the pyridyl nitrogen atoms adopt the expected transoid arrangement about the interannular bonds. The C–C and C–N bond lengths within the aromatic rings are normal (in the ranges 1.373 ± 0.025 and 1.353 ± 0.007 Å respectively) as are the interannular C–C bond lengths (all in the range 1.48 ± 0.01 Å). The planar angles between the central and outer pyridyl rings are 2.7 and 7.4° for L^1(A) and 4.7 and 16.8° for L^1(B). The planar angle between the anilino and central pyridyl groups is 27.4 and 27.5° for L^1(A) and L^1(B) respectively, considerably more twisted than in 4′-phenyl-2,2′:6′,2″-terpyridine (phterpy, the corresponding interannular planar angle is 10.9°)[21] but less so than found in 4′-(2,5-dimethoxyphenyl)-2,2′:6′,2″-terpyridine (dmpterpy, 50.4°).[22]

Complexes. The analytical and electrospray mass spectral data for the complexes are consistent with their formulations (full data are listed in the Experimental section). Electrospray (ES) mass spectra of the monomeric complexes all showed strong peaks for the parent molecular ion, $[ML_2]^{2+}$ (L = L^1–L^4, L^9 or terpy) and weaker peaks for the $[ML_2(PF_6)]^+$ and $[ML]^{2+}$ ions. The ES-mass spectrum of each dimer showed peaks for the $[(terpy)Ru(L–L)Ru(terpy)]^{4+}$ parent ion, and for the parent

Table 2 Selected bond lengths (Å) and torsional angles (°) for compound L^1 with estimated standard deviations (e.s.d.s) in parentheses

N(1A)–C(1A)	1.359(2)	N(3A)–C(15A)	1.359(2)
N(1A)–C(5A)	1.346(2)	N(4A)–C(19A)	1.382(3)
N(2A)–C(6A)	1.354(3)	C(5A)–C(6A)	1.479(2)
N(2A)–C(10A)	1.358(3)	C(8A)–C(16A)	1.479(3)
N(3A)–C(11A)	1.346(2)	C(10A)–C(11A)	1.481(2)

N(1A)–C(5A)–C(6A)–N(2A)	−172.6(1)
N(2A)–C(10A)–C(11A)–N(3A)	173.0(1)
C(7A)–C(8A)–C(16A)–C(17A)	27.2(2)
C(9A)–C(8A)–C(16A)–C(21A)	27.4(2)
N(1B)–C(5B)–C(6B)–N(2B)	−176.4(1)
N(2B)–C(10B)–C(11B)–N(3B)	−164.2(1)
C(7B)–C(8B)–C(16B)–C(17B)	−26.0(2)
C(9B)–C(8B)–C(16B)–C(21B)	−29.0(2)

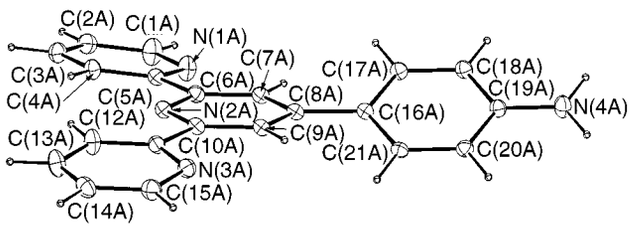

Fig. 3 An ORTEP[20] plot of L^1 (molecule A; 20% thermal ellipsoids for non-hydrogen atoms)

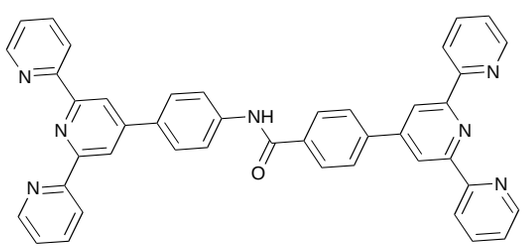

L–L' = L^{10}

ion–counter anion cluster ions, $[(terpy)Ru(L–L)Ru(terpy) + PF_6]^{3+}$ and $[(terpy)Ru(L–L)Ru(terpy) + 2PF_6]^{2+}$.

For the polymers, $[\{Fe(L–L)\}_n][BF_4]_{2n}$ (L–L = L^5–L^7), ES and matrix-assisted-laser-desorption-ionisation time-of-flight (MALDI-TOF) mass spectra were unrevealing as to the overall polymer molecular weight. The highest mass peak in MALDI-TOF mass spectra of the three polymers $[\{Fe(L–L)\}_n][BF_4]_{2n}$ prepared by route (*b*) was for the $[Fe(L–L)_2]^+$ ion and no peaks for $[FeL^1_2]^{2+}$ or $[FeL^1_2]^+$ ions were observed. Two conclusions can be made. (*i*) The complex $[FeL^1_2]^{2+}$ is completely consumed in the condensation reactions and results in species with the corresponding binucleating bis(terpyridyl) ligands, L^5–L^7. (*ii*) Oligomeric ions are not observed, presumably these fragment during the desorption-ionisation process because the co-ordinate bonds to the first-row transition metal, iron(II), ion are relatively weak and labile. Some independent support for this conclusion comes from the MALDI-TOF mass spectra of oligomers of L^{10}.[22] For example, in MALDI-TOF mass spectrum of $[(terpy)Ru(L–L')Fe(L'–L)Ru(terpy)][PF_6]_6$ (L–L' = L^{10}) by far and away the most intense peak is at *m/z* 993 for the $[Ru(terpy)L^{10}]^{2+}$ fragment ion with peaks for the molecular ion, M^{6+}, and molecular ion–counter anion cluster ions, $[M + nPF_6]^{(6-n)+}$, being either very weak or not observed (depending on conditions).

Estimates of average polymer molecular weights can sometimes be made from gel permeation chromatography (GPC) measurements or from NMR detection of end-caps following end-capping experiments.[1,23] Unfortunately, meaningful GPC measurements could not be obtained because GPC standards appropriate for the rigid-rod polycations, $[\{Fe(L–L\}_n]^{2n+}$, are not available and the polymers were insoluble in lower-boiling-point solvents that are typically used for these measurements.[1,23] However, the condensation of $[FeL^1_2][BF_4]_2$ with pyromellitic dianhydride with pyridine as the base to give $[(FeL^5)_n][BF_4]_{2n}$ could be quenched by addition of an excess of acetyl chloride forming acetamide end-groups, thereby allowing ^{1}H NMR spectroscopic determination of the average degree of polymerisation (DP). Independently, $[FeL^1_2][BF_4]_2$ was treated with acetyl chloride and formation of the bis(4′-phenylacetamide) end-capped complex was shown to be quantitative within detectable limits by ^{1}H NMR spectroscopy. A DP of 17.2 for $[(FeL^5)_n][BF_4]_{2n}$ which corresponds to an average molecular weight of 18 200 was obtained when the polymerisation was quenched after 16 h. It should be noted that end-capping experiments only give a lower estimate of the DP and average molecular weight.

Linear rigid-rod structures are favoured by the bonding and by the steric and electrostatic interactions in the polycations, $[(FeL^5)_n]^{2n+}$. The length of the repeat unit is estimated to be about 27.5 Å {using the sum of the distance between the two anilino nitrogen atoms in $[CuL^1_2]^{2+}$ (determined by X-ray crystallography at 20.84 Å, see below) and 6.70 Å for the distance between the nitrogen atoms in diphenylpyromellitimide (*N*,*N*′-diphenylbenzene-1,2:4,5-dicarboximide)}. The cylindrical, rigid-rod polycations, $[(FeL^5)_n]^{2n+}$, with a DP of 17.2 thus have an average length of about 473 Å and a radius of 5.8 Å (the distance between the metal centre and the periphery of the terpyridyl ligands).

Table 3 Selected bond lengths (Å) and angles (°) for $[CuL^1_2][PF_6]_2$ with e.s.d.s in parentheses

Cu–N(1A)	2.154(6)	Cu–N(1B)	2.184(6)
Cu–N(2A)	1.972(5)	Cu–N(2B)	1.986(5)
Cu–N(3A)	2.136(6)	Cu–N(3B)	2.180(6)
C(19A)–N(4A)	1.373(8)	C(19B)–N(4B)	1.393(9)
N(1A)–Cu–N(2A)	76.5(2)	N(2A)–Cu–N(3B)	107.1(2)
N(1A)–Cu–N(3A)	155.3(2)	N(3A)–Cu–N(1B)	91.2(2)
N(1A)–Cu–N(1B)	91.7(2)	N(3A)–Cu–N(2B)	103.1(2)
N(1A)–Cu–N(2B)	101.4(2)	N(3A)–Cu–N(3B)	94.7(2)
N(1A)–Cu–N(3B)	93.2(2)	N(1B)–Cu–N(2B)	77.7(2)
N(2A)–Cu–N(3A)	78.8(2)	N(1B)–Cu–N(3B)	154.5(2)
N(2A)–Cu–N(1B)	98.4(2)	N(2B)–Cu–N(3B)	76.8(2)
N(2A)–Cu–N(2B)	175.6(2)		
C(18A)–C(19A)–N(4A)	121.4(8)	C(18B)–C(19B)–N(4B)	120.3(9)
N(4A)–C(19A)–C(20A)	120.8(8)	N(4B)–C(19B)–C(20B)	120.4(9)

Crystal structure of $[CuL^1_2][PF_6]_2$. Green crystals of $[CuL^1_2][PF_6]_2$ deposited from a solution of the complex in acetone–methanol under an atmosphere of diethyl ether vapour. The molecular structure of the cation and numbering scheme adopted is depicted in Fig. 4 and selected bond angle and length data are presented in Table 3.

The structure analysis revealed that $[CuL^1_2][PF_6]_2$ crystallised in the space group $P2_12_12_1$ with four cations and eight anions, all well separated from each other, in the unit cell. The copper(II) ion displays the expected distorted-octahedral geometry with intraligand bite angles in the range 76.5–78.8°. The planar angle between central pyridyl rings of the two terpyridyl ligands is 89.5° and the angle formed by the Cu atom and the nitrogen atoms of the central pyridyl groups [N(2A)–Cu–N(2B)] is 175.6(2)°. All C–N and C–C distances are in the normal range. The most notable feature of the structure is that the two terpyridyl ligands, A and B, are inequivalent and show different binding to the copper ion. The two Cu–N (central pyridyl ring) distances are similar at 1.972(5) (ligand A) and 1.986(5) (B), but Cu–N (terminal pyridyl ring) distances for the two ligands are significantly different, with those to ligand B [average 2.182(6) Å] elongated compared to those for A [average 2.154(6) Å]. The same orthorhombic distortion from octahedral symmetry is observed in $[Cu(terpy)_2][NO_3]_2$[24] and $[Cu(dmpterpy)_2][BF_4]$,[22]

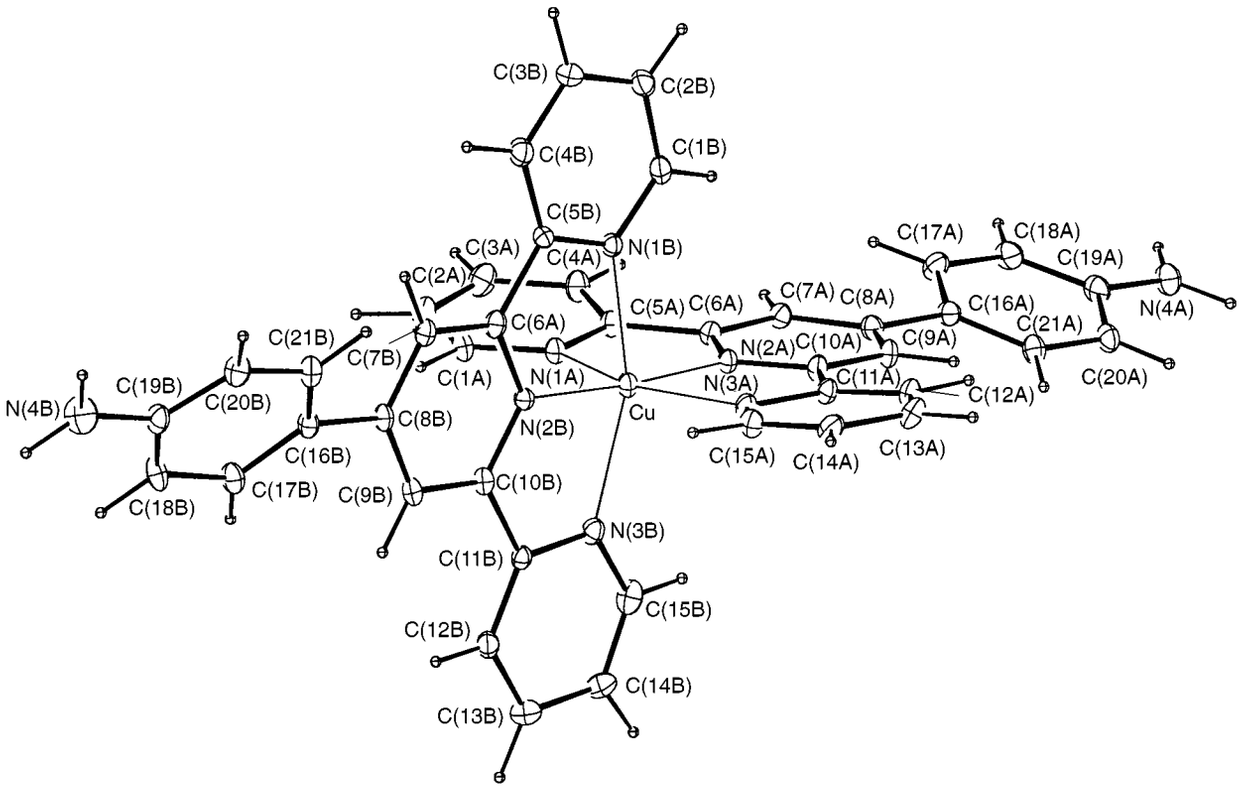

Fig. 4 An ORTEP plot of the cation $[CuL^1_2]^{2+}$ (20% thermal ellipsoids for non-hydrogen atoms)

and has been attributed to the compromise between tetragonal compression along the axis roughly defined by N(2A), Cu and N(2B) as a result of the rigid terpyridine ligands and a tetragonal elongation along the axis roughly defined by N(1B), Cu and N(3B) as a consequence of the Jahn–Teller effect.[24] The inequivalence of the two terpyridyl ligands is also revealed by the planar angles (and interannular distances) between the central pyridyl and anilino rings within each ligand [17.8° (1.468 Å) for ligand A and 38.2° (1.503 Å) for B]. The corresponding interannular twist and distance in free L^1 (see above) lie midway between those observed for ligands A and B in the $[CuL^1_2]^{2+}$ cation. This suggests that, compared to free L^1, the π overlap between the central pyridyl and anilino rings is increased in ligand A and decreased in B.

Magnetism and NMR spectroscopy. The complexes $[ML^1_2]^{2+}$ (M = Mn, Co, Ni or Cu) are paramagnetic and Table 4 lists both the solution magnetic moment data ascertained using the Evans method[25] and the ambient-temperature solid-state data. The magnetic moment data for the complexes Mn^{II}, Ni^{II} and Cu^{II} agree with expected values for high-spin octahedral complexes. The magnetic moment of $[CoL^1_2][PF_6]_2$ in acetone solution varied significantly with temperature as shown in Fig. 5. Octahedral cobalt(II) complexes show magnetic moments in the range 4.8–5.2 μ_B for high-spin complexes and 2.0–2.5 μ_B for low-spin complexes. The intermediate and decreasing values for the $[CoL^1_2]^{2+}$ ion over the temperature range 310 (μ_{eff} = 3.67) to 210 K (2.61 μ_B) are consistent with an incomplete, broad continuous spin transition. Other bis(terpyridyl)cobalt(II) complexes show similar magnetic behaviour.[7]

Proton NMR data for the diamagnetic complexes are summarised in Table 5. The monomeric complexes, $[ML_2]^{2+}$ (L = L^1, M = Fe, Ru or Zn; L = L^2–L^4, M = Fe; L = L^9, M = Fe or Zn), $[RhL^1_2]^{3+}$ and $[Ru(terpy)L]^{2+}$ (L = L^1–L^4 or L^9), and the dimers, $[(terpy)Ru(L–L)Ru(terpy)]^{4+}$ (L–L = L^5–L^7), gave ^1H NMR spectra that agree with their indicated structures. Assignments of the ^1H NMR spectra were easily made with the aid of double quantum filtered correlation (DQF-COSY) ^1H–^1H NMR spectra of selected complexes and using comparisons with the ^1H NMR spectra reported for other ruthenium(II) complexes of 4′-substituted terpyridyl ligands.[11,26] As examples of assigned ^1H NMR spectra, those for the dimers are shown in Fig. 6. Notable features from the ^1H NMR spectra are: (*i*) as expected, protons H^6 closest to the metal centre are most affected as the metal centre is changed in the $[ML^1_2]^{n+}$ complexes {*e.g.* δ(H^6) is 7.55 for $[FeL^1_2]^{2+}$ whereas δ(H^6) is 8.30 for $[RhL^1_2]^{3+}$}; (*ii*) in the

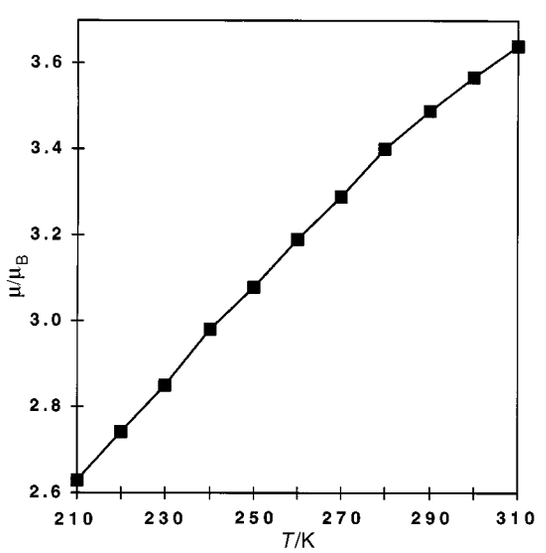

Fig. 5 Temperature-dependent magnetic moment data for $[CoL^1_2][PF_6]_2 \cdot 2H_2O$ in acetone solution

Table 4 Magnetic moments (μ_B) at 295 K

Complex	Acetone solution	Solid state
$[CoL^1_2][PF_6]_2$	3.34	3.23
$[CuL^1_2][PF_6]_2$	2.36	2.07
$[MnL^1_2][PF_6]_2$	5.97	6.35
$[NiL^1_2][PF_6]_2$	3.34	3.41

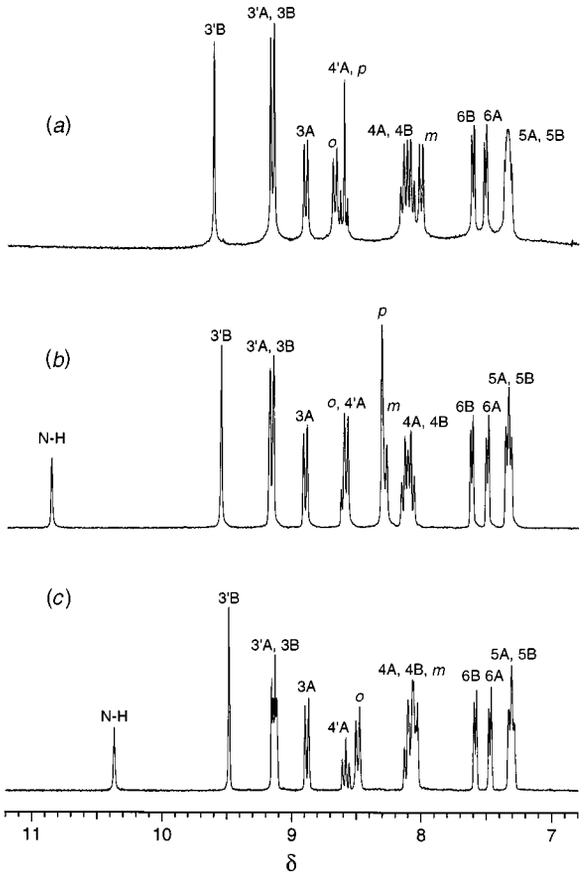

Fig. 6 The 300 MHz ^{1}H NMR spectra of the dimers, [(terpy)Ru(L–L)-Ru(terpy)]$^{4+}$, recorded in $(CD_3)_2SO$: L–L = L^5 (*a*), L^6 (*b*) and L^7 (*c*)

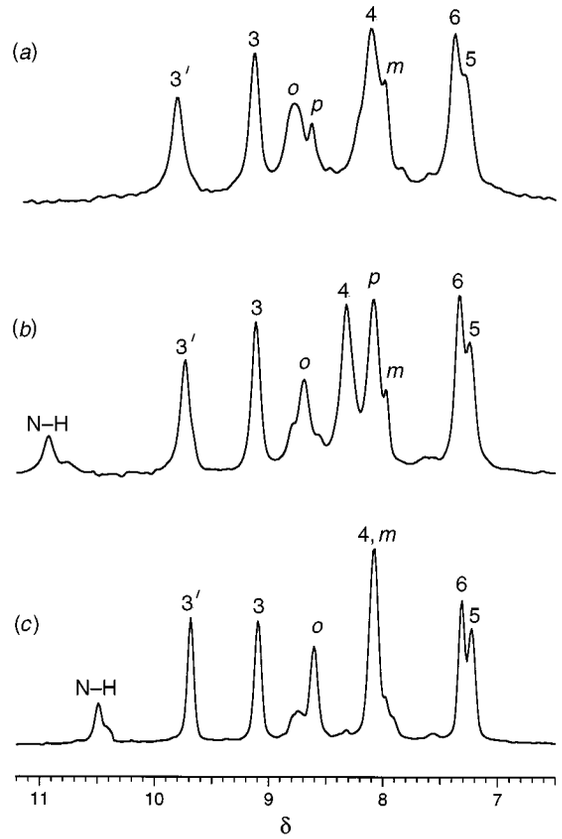

Fig. 7 The 300 MHz ^{1}H NMR spectra recorded in $(CD_3)_2SO$ of the polymers, [{Fe(terpy)(L–L)}$_n$][BF_4]$_{2n}$: L–L = L^5 (*a*), L^6 (*b*) and L^7 (*c*)

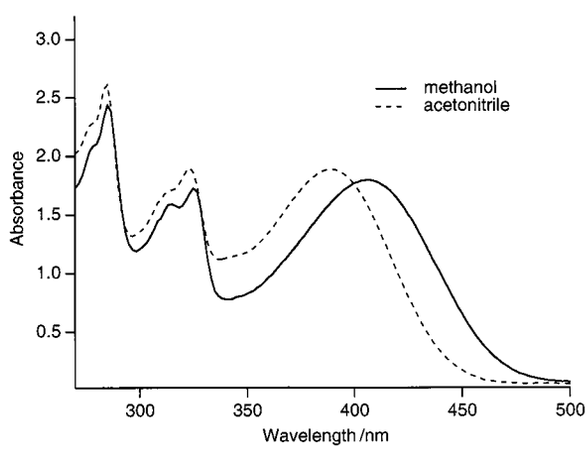

Fig. 8 The UV/VIS spectra of [ZnL^1_2][PF_6]$_2$

[ML^1_2]$^{n+}$ complexes, the largest co-ordination changes in chemical shift ($\Delta\delta = \delta_{complex} - \delta_{free\ ligand}$) were for the NH_2 protons ($\Delta\delta$ varied from 1.51 to 1.93 ppm) followed by the H^6 protons ($\Delta\delta$ varied from −0.33 to −1.18 ppm) and $H^{3'}$ protons ($\Delta\delta$ varied from 0.52 to 0.78 ppm) with the magnitudes $|\Delta\delta|$ for all other protons being less than 0.4 ppm; (*iii*) in the heteroleptic complexes, independent peaks are observed for both terpyridyl domains; and (*iv*) in complexes of L^1, the two peaks for the NH_2 protons likely result from facile exchange of these protons with the deuteriated solvent to give the isotopomers, NH_2 (observed, one peak), NHD (observed, one peak) and ND_2 (not observed). Both peaks were lost on shaking with D_2O. In some ^{13}C-{^{1}H} NMR spectra less than the requisite number of peaks for magnetically non-equivalent carbon atoms were observed. This is attributed to chemical shift coincidence of some of the peaks. Finally, the ^{1}H NMR spectra of the polymeric cations [{Fe(L–L)}$_n$]$^{2n+}$ (L–L = L^5–L^7) reveal the correct number of broad peaks at positions roughly corresponding to the chemical shift of the analogous protons in the ^{1}H NMR spectra of the [FeL_2]$^{2+}$ (L = L^2–L^4) model compounds (compare Figs. 6 and 7). Broadening of the peaks is expected for the polymeric cations due to the decreased mobility and increased correlation times in solution.[23]

Colour and absorption spectra. Owing to their potential as pigments for incorporation into macromolecules the colours of the complexes are of some interest. They cover a large portion of the visible spectrum. For example, the [ML^1_2]$^{n+}$ complexes range from intense red (Ru^{II}), dark orange (Rh^{III}), yellow-brown (Ni^{II}), yellow (Mn^{II}), through pale yellow (Zn^{II}) and green (Cu^{II}) to maroon (Co^{II}) and deep purple (Fe^{II}).

Data from UV/VIS spectra of the complexes are presented in Table 1. The complexes [ML^1_2]$^{2+}$ (M = Mn, Ni, Cu or Zn) show the same bands as free L^1 (see above) but with about twice the intensity, *e.g.* Fig. 8. These bands and weak d–d bands contribute to the observed colours of the complexes. The weak bands shown in Fig. 9 in the visible or near-infrared regions of spectra for the complexes [ML^1_2]$^{2+}$ (M = Co, Ni or Cu) are attributed to d–d transitions by comparison with literature assignments for analogous terpy or phterpy complexes.[6–9,21] In absorption spectra of L^1 and its complexes the lowest-energy ligand-centred band at ≈405 nm is solvatochromic, shifting in energy with solvent. For example, spectra of [ZnL^1_2]$^{2+}$ in methanol and acetonitrile are reproduced in Fig. 8. This behaviour was not investigated further because of the poor solubility of L^1 and its complexes in less polar solvents. The intense ligand-centred band at *ca.* 495 nm in the UV/VIS spectra of L^9 and its complexes also shifts in energy (±10 nm) with solvent.

The visible regions of the absorption spectra of the iron, ruthenium, cobalt and rhodium complexes are dominated by intense charge-transfer bands and there are accompanying

Table 5 The 300 MHz ^{1}H NMR data (δ) for the diamagnetic complexes

	terpy derivative									terpy					
Compound	$H^{3'}$	H^3	H^4	H^5	H^6	H^o	H^m	NH	Other	$H^{3'}$	$H^{4'}$	H^3	H^4	H^5	H^6
L^1 [a]	8.69	8.66	7.87	7.34	8.73	7.78	6.80	3.89							
$[FeL^1_2][BF_4]_2$ [b]	9.47	8.97	8.03	7.24	7.55	8.26	7.03	5.48, 5.47							
$[RhL^1_2][PF_6]_2$ [b]	9.42	9.17	8.42	7.63	8.30	8.21	6.99	5.82, 5.81							
$[RuL^1_2][PF_6]_2$ [b]	9.28	9.00	8.06	7.32	7.79	8.13	6.98	5.41, 5.39							
$[ZnL^1_2][PF_6]_2$ [b]	9.21	9.06	8.27	7.52	8.17	8.17	6.98	5.53, 5.52							
$[FeL^2_2][BF_4]_2$ [c]	9.79	9.12	8.11	7.27	7.36	8.74	7.99		8.11, 8.04						
$[FeL^3_2][BF_4]_2$ [c]	9.75	9.14	8.09	7.24	7.34	8.68	8.31	10.78	8.13, 7.72, 7.66						
$[FeL^4_2][BF_4]_2$ [c]	9.67	9.08	8.06	7.22	7.31	8.57	8.06	10.40	2.78						
$[FeL^9_2][BF_4]_2$ [b]	9.63	9.00	8.04	7.22	7.55	8.51	7.83		6.16, 6.01, 4.13, 1.41						
$[ZnL^9_2][PF_6]_2$ [b]	9.33	9.04	8.04	7.47	8.16	8.35	7.73		6.08, 5.95, 4.06, 1.35						
$[Ru(terpy)L^1][PF_6]_2$ [b]	9.28	8.99	8.06	7.32	7.66	8.13	6.98	5.41, 5.40		9.06	8.54	8.80	8.08	7.34	7.81
$[Ru(terpy)L^2][PF_6]_2$ [b]	9.45	9.03	8.04	7.30	7.69	8.40	7.88		8.01, 7.95	9.06	8.55	8.78	8.04	7.30	7.78
$[Ru(terpy)L^3][PF_6]_2$ [c]	9.36	9.16	8.07	7.32	7.47	8.56	8.26	10.59	8.11, 7.66, 7.64	9.16	8.57	8.91	8.11	7.32	7.69
$[Ru(terpy)L^4][PF_6]_2$ [b]	9.35	8.98	8.03	7.28	7.66	8.25	7.96	9.50	2.78	9.03	8.53	8.77	8.03	7.28	7.76
$[Ru(terpy)L^9][PF_6]_2$ [b]	9.41	9.01	8.04	7.29	7.68	8.39	7.77		6.11, 6.00, 4.11, 1.40	9.05	8.55	8.78	8.04	7.30	7.77
$[(terpy)RuL^5Ru(terpy)][PF_6]_4$ [c]	9.62	9.16	8.12	7.34	7.52	8.68	8.01		8.60	9.16	8.60	8.91	8.12	7.34	7.61
$[(terpy)RuL^6Ru(terpy)][PF_6]_4$ [c]	9.16	9.55	8.11	7.33	7.49	8.60	8.28	10.85	8.28	9.16	8.60	8.90	8.11	7.33	7.61
$[(terpy)RuL^7Ru(terpy)][PF_6]_4$ [c]	9.16	9.55	8.11	7.33	7.49	8.60	8.28	10.38	2.59, 1.88	9.15	8.59	8.89	8.07	7.31	7.59

[a] Recorded in $CDCl_3$. [b] Recorded in $(CD_3)_2CO$. [c] Recorded in $(CD_3)_2SO$.

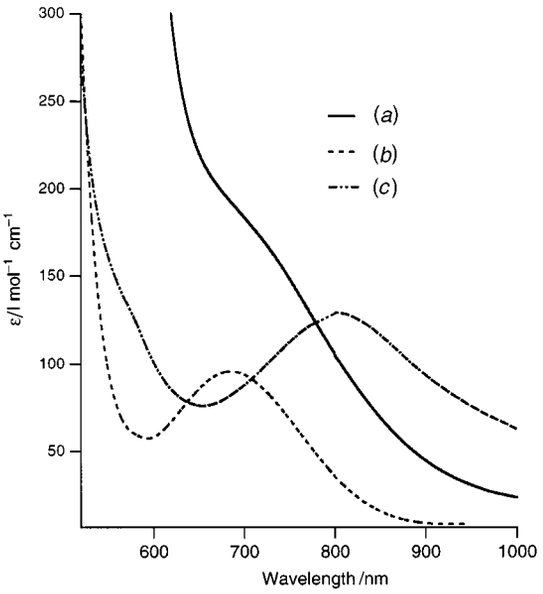

Fig. 9 The VIS/NIR spectra in acetone for (*a*) $[CoL^1_2][PF_6]_2$, (*b*) $[NiL^1_2][PF_6]_2$ and (*c*) $[CuL^1_2][PF_6]_2$

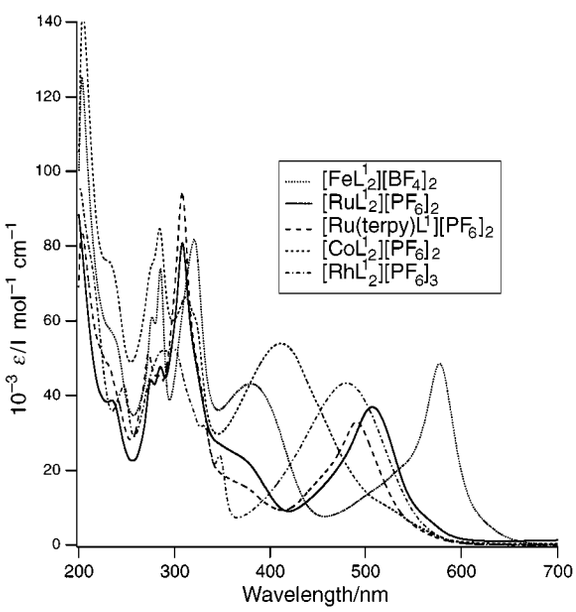

Fig. 10 The UV/VIS spectra of listed complexes in methanol solution

changes in the relative intensities of the ligand-centred bands, *e.g.* Fig. 10. The intense bands in the visible region for the iron and ruthenium complexes are the result of spin-allowed $d_\pi(M) \longrightarrow \pi^*$(terpy), metal-to-ligand charge-transfer (^{1}MLCT) transitions.[8,10] The MLCT bands of the iron and ruthenium complexes are all red-shifted and considerably more intense than the MLCT bands observed for $[Fe(terpy)_2]^{2+}$ and $[Ru(terpy)_2]^{2+}$. This red-shift is small (≤15 nm) and reproducibly larger for complexes of L^1 (by ≈6 nm) than for complexes of the imido or amido functionalised ligands, L^2–L^7. Red-shifted MLCT band maxima are characteristic of bis(terpyridyl)ruthenium(II) complexes with the ligands substituted at the 4′-positions by either donor or acceptor groups. The effect arises because electron-accepting groups stabilise the π*(terpy) lowest unoccupied molecular orbital (LUMO) more than the d_π metal highest occupied molecular orbital (HOMO) whereas electron-donating groups cause a larger destabilisation of the d_π metal HOMO than the π*(terpy) LUMO.[8] The MLCT band maxima are thus consistent with the anilino group in L^1 being a better donor group than the benzimido or the benzamido groups in L^2–L^7.

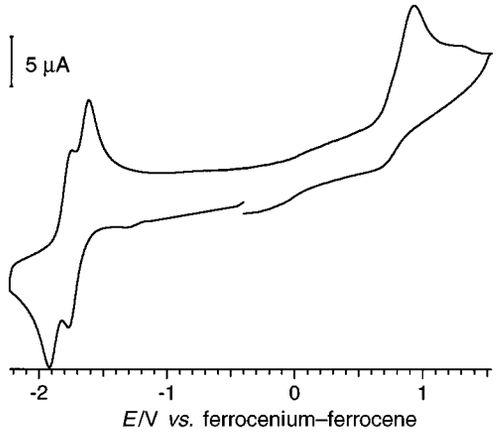

Fig. 11 Cyclic voltammogram of $[ZnL^1_2][PF_6]_2$ in acetonitrile–0.1 mol l^{-1} $[NBu^n_4][PF_6]$ at a platinum-disc working electrode (scan rate 100 mV s^{-1})

Electrochemical behaviour. The voltammetric behaviour of the ligands (Table 6) and the complexes (Tables 7 and 8) was probed by cyclic and differential pulse voltammetries.

Cyclic voltammograms of ligand L^1 in acetonitrile solution show an irreversible oxidation process at +0.88 V and no other distinct processes over the potential range +2.0 to −2.3 V. Bulk electrolysis revealed the oxidation to be a two-electron process. Given the absence of such an oxidation process in phterpy,[21] it seems likely that the process is centred on the anilino-group. Under analogous aprotic conditions, aniline also displays an irreversible two-electron oxidation (at ≈+0.66 V).[27] We assume that the anticipated one-electron reduction of the terpyridyl centre takes place at potentials negative of −2.3 V.

Each monomeric complex shows the voltammetric responses expected for the respective $M(terpy)_2^{n+}$ core, typically M^{III}–M^{II} and/or M^{II}–M^{I} couples and two terpyridyl-centred reduction processes {the $[M(terpy)_2]^{n+}$–$[M(terpy)(terpy^-)]^{(n-1)+}$ and $[M(terpy)(terpy^-)]^{(n-1)+}$–$[M(terpy^-)_2]^{(n-2)+}$ couples}. The voltammetric responses for the $[M(terpy)_2]^{n+}$ cores are relatively well known[9] and, rather than detailed description, assignments are summarised in Table 6. In addition to the $[M(terpy)_2]^{n+}$ core processes, an irreversible anilino-centred oxidation was observed between +0.62 to +0.92 V for the complexes $[ML^1_2]^{n+}$, *e.g.* Fig. 11. Complexes of the phthalimido-ligand L^2 and amido-ligands L^3, L^4 showed irreversible oxidations at ≈+1.5 V. A phthalimido-centred reduction couple at ≈−1.8 V was also observed for complexes of L^2. Since the oxidation of the anilino-group precedes the M^{III}–M^{II} couple in the iron and ruthenium complexes, the influence of the anilino-group on these couples cannot be judged. However, comparison of the Co^{III}–Co^{II} and Co^{II}–Co^{I} couples for $[CoL^1_2]^{2+}$ ($E_{\frac{1}{2}}$ = −0.24 and −1.25 V) with those for $[Co(phterpy)_2]^{2+}$ ($E_{\frac{1}{2}}$ = −0.15 and −1.20 V)[28] and $[Co(terpy)_2]^{2+}$ ($E_{\frac{1}{2}}$ = −0.13 and −1.18 V)[28] reveals that the donor anilino moiety stabilises the higher oxidation state in each couple. Cyclic voltammograms of L^9 and its complexes show an anodic peak at ≈+1.1 V ascribed to irreversible oxidation of the anilinoquinone group(s) (for comparison, 2-anilino-1,4-benzoquinine shows an irreversible oxidation process at ≈+1.4 V[17,18]). Not all of the $[M(terpy)_2]^{n+}$ core processes anticipated for the complexes of L^9 could be assigned (Table 7) because cyclic voltammograms to potentials negative of ≈−1.0 V were dominated by complicated adsorption and stripping peaks.

Cyclic voltammograms of the dimers $[(terpy)Ru(L–L)Ru(terpy)]^{4+}$ (L–L = L^5–L^7) have been published in a preliminary communication[15] and data are given in Table 8. Each of the dimers shows a combination of the redox processes expected for two electrochemically isolated $[Ru(terpy)(terpy^-)]^{2+}$ centres (one Ru^{III}–Ru^{II} couple at ≈+0.9 V and two terpy–terpy$^-$ couples at approximately −1.7 and −1.9 V, each with a two-electron peak current) and for the intervening organic linkage[13]

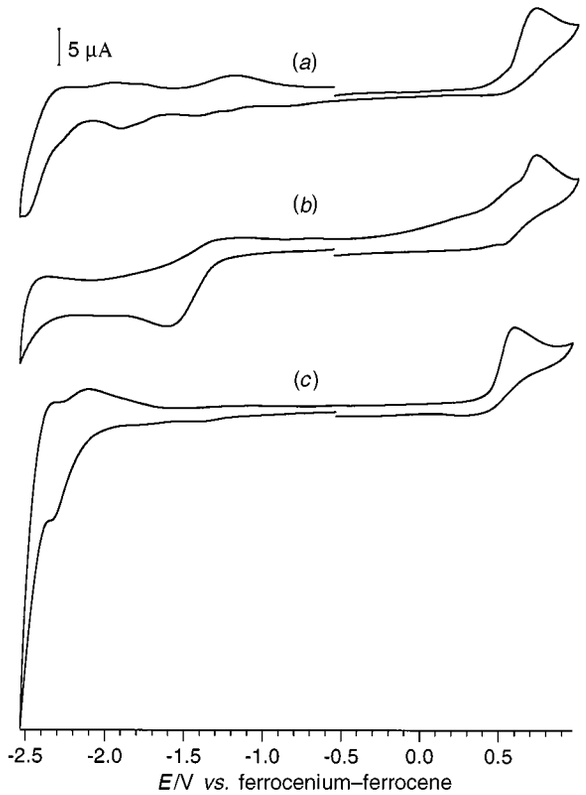

Fig. 12 Cyclic voltammograms in acetonitrile–0.1 mol l^{-1} $[NBu^n_4][PF_6]$ at a platinum-disc working electrode (scan rate 100 mV s^{-1}) or the polymers, $[\{Fe(L–L)(terpy)\}_n][BF_4]_{2n}$: L–L = L^5 (*a*), L^6 (*b*) and L^7 (*c*)

$\{[(terpy)RuL^5Ru(terpy)]^{4+}$: an irreversible oxidation at +0.65 V and two reversible one-electron reductions centred at the pyromellitimido linkage at −1.13 and −1.79 V; $[(terpy)RuL^6Ru(terpy)]^{4+}$: irreversible oxidation of the terephthalamido linking group at ≈+0.9 V (overlaps with the Ru^{III}–Ru^{II} couple); $[(terpy)RuL^7Ru(terpy)]^{4+}$: irreversible amido-centred oxidation at +0.65 V}.

In cyclic voltammograms of the polymers, Fig. 12, the Fe^{III}–Fe^{II} couples and irreversible imido- or amido-oxidation processes merge to give poorly reversible oxidation features at ≈+0.63 V. Distinct terpyridine-centred reduction couples are no longer observed. Rather, the cyclic voltammograms of the three polymers reveal a poorly reversible reduction process at ≈−2.3 V (near the cathodic solvent discharge). The complex $[(FeL^7)_n]^{2n+}$ also exhibits a broad irreversible reduction at −1.55 V. The reason(s) for the poor reversibility of the electrochemical responses of the polymers is not well understood. Similar poorly reversible electrochemical behaviour is exhibited by dendrite-coated bis(terpyridine)-iron(II) and -ruthenium(II) complexes.[29] The irreversibility of the electrochemical processes in these systems was attributed to inhibition of electron transfer between the electrode and the metal centres by the insulating dendritic coating. We speculate that the morphologies of the $[\{Fe(L–L)\}_n]^{2n+}$ polycations may prevent close approach of most of the redox centres in each polycation to the electrode thereby providing a barrier to electron transfer between the electrode and the redox centres.

Conclusion

These results reveal transition-metal complexes of L^1 to be readily obtainable and to display a wide variety of chromophoric, magnetic and electrochemical properties. The model reactions demonstrate that the pendant aniline groups in complexes of L^1 can be readily functionalised using standard organic synthetic methods, and techniques for preparations of metallodimers and metallopolymers using L^1 and its complexes have been developed. The failure of the complexes of L^1 to react with benzoquinone suggests a potential limitation, lower than usual nucleophilicity for the anilino group in these systems. Nevertheless, we believe that straightforward extensions of the successful syntheses described herein should provide a wide variety of interesting multicomponent bis(terpyridyl) transition-metal systems for future studies.

Table 6 Electrochemical data for the ligands; potentials (V) are *versus* the ferrocenium–ferrocene couple

		Oxidation	Reduction		
Ligand	Solvent[a]	E_a	E_1	E_2	E_3
L^1	MeCN	0.88[b]			
L^2	MeCN	1.93[b]		−1.79[c]	−2.36
L^3	dmf	0.61[b]	−0.84[b,d]		−2.58
L^6	dmf	0.65[b]	−0.88[b,d]	−2.25	−2.73
L^9	MeCN	1.0[b]			

[a] Solvent containing 0.1 mol l^{-1} $[NBu^n_4][PF_6]$. [b] Irreversible process. [c] Imide-centred reduction. [d] Coupled with E_a.

Experimental

All reactions were carried out under an atmosphere of dry dinitrogen unless otherwise stated, using standard Schlenk and cannula techniques. Solvents were routinely distilled from an appropriate drying agent immediately prior to use. Acetonitrile was distilled from calcium hydride; dmf was dried over calcium hydride and then distilled under reduced pressure; methanol and ethanol were distilled from magnesium turnings, nmp was distilled from phosphorus pentaoxide; pyridine was distilled from barium oxide and stored over barium oxide under dinitrogen. Anhydrous dma stored under an inert atmosphere was purchased from Aldrich Chemical company and used as received. Acetone was distilled from potassium permanganate and then from boric oxide. The solvents used for electrochemical measurements, acetonitrile and dimethylformamide, were highest-quality anhydrous grade sealed under argon (Aldrich) and were used as obtained.

Flash chromatography was carried out using Merck silica gel 7730 $60GF_{254}$. Columns were packed with dry gel; solvent was applied to the column before a concentrated solution of the sample in the appropriate solvent. A water aspirator was attached to the receiving flask during packing and elution. Quoted melting points are uncorrected. Microanalyses (for C, H and N) were performed by the University of New South Wales microanalytical service. Prior to analysis, samples were dried at 40 °C for 48 h under vacuum (0.2 mmHg) over phosphorus pentaoxide. Electron ionisation and electrospray mass spectra were recorded using a VG Quattro mass spectrometer and matrix-assisted-laser-desorption-ionisation time-of-flight mass spectra were recorded on a Finnigan Lasermat instrument using a matrix of either α-cyano-4-hydroxycinnamic acid or sinapinic acid $[HOC_6H_2(OMe)_2CH{=}CHCO_2H]$. Proton and ^{13}C NMR spectra were obtained in the designated solvents on a Bruker AC-F 300 (300 MHz) instrument, infrared spectra as Nujol mulls on a Perkin-Elmer 580B spectrometer (only the most prominent peaks are reported) and electronic spectra using a CARY 5 spectrophotometer in the dual-beam mode. Solution measurements of magnetic moments were determined in acetone solution using the Evans method[25] on a Bruker AC-F 300 (300 MHz) NMR spectrometer. Electrochemical measurements were recorded using a Bioanalytical Systems (BAS) 100B Electrochemical Analyser interfaced to a 486 IBM-compatible personal computer. Data were transferred to a Macintosh Power PC 7600 computer for processing using the IGORPRO 2.0™ software.[30] Cyclic and differential pulse voltammetries were conducted in a standard three-electrode cell

Table 7 Electrochemical data for the monomeric complexes in MeCN containing 0.1 mol l^{-1} $[NBu^n_4][PF_6]$; potentials (V) are *versus* the ferrocenium–ferrocene couple

Complex	M^{II}–M^{III}	M^{II}–M^{I}	E_a	E_1	E_2	E_3
$[CoL^1_2]^{2+}$	−0.24	−1.25	0.77	−2.08		
$[CuL^1_2]^{2+}$		−0.72	0.82			
$[MnL^1_2]^{2+}$			0.82	−1.54	−1.81	
$[NiL^1_2]^{2+}$			0.72	−1.75	−1.93	
$[RhL^1_2]^{3+}$		−1.06 [a]	0.85			
$[RuL^1_2]^{2+}$	0.96		0.74	−1.70	−1.94	
$[ZnL^1_2]^{2+}$			0.92	−1.70	−1.84	
$[FeL^1_2]^{2+}$	0.69		0.62	−1.70	−1.78	
$[FeL^2_2]^{2+}$	0.69		1.54	−1.60	−1.71	−1.81 [b]
$[FeL^3_2]^{2+}$	0.68		1.45	−1.66	−1.78	−1.44 [c]
$[FeL^4_2]^{2+}$	0.68		1.54	−1.64	−1.73	
$[Ru(terpy)L^1]^{2+}$	0.91		0.63	−1.68	−1.93	
$[Ru(terpy)L^2]^{2+}$	0.88		1.87	−1.63	−1.91	−2.43 [d]
$[Ru(terpy)L^3]^{2+}$	0.86		1.36	−1.68	−1.95	−2.44 [d]
$[Ru(terpy)L^4]^{2+}$	0.86		1.45	−1.65	−1.90	−2.44 [d]
$[CoL^9_2]^{2+}$	−0.15		1.27			
$[FeL^9_2]^{2+}$	0.68		1.23			
$[ZnL^9_2]^{2+}$			1.26			
$[Ru(terpy)L^9]^{2+}$	0.89		1.12			

E_a = Irreversible oxidation process; E_1, E_2 = first and second terpyridyl-centred reduction couples. [a] Rh^{III}–Rh^{I} couple. [b] Imide-centred reduction. [c] Coupled with E_a. [d] Data from differential pulse voltammetry.

Table 8 Electrochemical data for the ruthenium(II) dimers and iron(II) polymers in dmf containing 0.1 mol l^{-1} $[NBu^n_4][PF_6]$; potentials (V) are *versus* the ferrocenium–ferrocene couple

Complex	M^{II}–M^{III}	E_a	E_1	E_2	E_3
$[(terpy)RuL^5Ru(terpy)]^{4+}$	0.78	0.65	−1.68	−1.92	−1.13, [a] −1.79 [a]
$[(terpy)RuL^6Ru(terpy)]^{4+}$	0.9 [b]		−1.68	−1.92	−0.85 [c]
$[(terpy)RuL^7Ru(terpy)]^{4+}$	0.79	0.65	−1.67	−1.91	−0.81 [c]
$[Ru(terpy)L^1]^{2+}$	0.82	0.58	−1.70	−1.92	
$[(FeL^5)_n]^{2n+}$	0.63				
$[(FeL^6)_n]^{2n+}$	0.63				
$[(FeL^7)_n]^{2n+}$	0.61				

E_a = Irreversible oxidation; E_1 and E_2 = first and second terpy-core reductions. [a] Imide-centred reduction. [b] Overlap of irreversible amide oxidation and Ru^{II}–Ru^{III} couple. [c] Coupled with E_a.

consisting of a platinum-disc working electrode (0.8 mm diameter, BAS), platinum-wire (0.05 mm diameter) auxiliary electrode and a Ag–AgCl reference electrode (BAS). All potentials are quoted relative to the ferrocenium–ferrocene couple which was measured *in situ* as an internal reference.

Preparations

3-(4-Anilino)-1,5-bis(2-pyridyl)pentane-1,5-dione. Freshly prepared *p*-aminobenzaldehyde (4.46 g, 36.8 mmol) was dissolved in ethanol (250 cm^3) and NaOH (3.0 g) in water (30 cm^3) added. 2-Acetylpyridine (8.5 cm^3, 80 mmol) was added dropwise and the solution stirred at room temperature for 80 h. During this period a precipitate formed and this was filtered off and washed with water then diethyl ether. The crude product was recrystallised from ethanol to give a yellow-brown microcrystalline solid (3.21 g, 20%), m.p. 153–155 °C (Found: C, 72.93; H, 5.78; N, 12.00. Calc. for $C_{21}H_{19}N_3O_2$: C, 73.04; H, 5.51; N, 12.17%). EI mass spectrum: *m/z* 345 (M^+). ^{1}H NMR ($CDCl_3$): δ 8.63 (d, 2 H, J = 4.6, H^6), 7.93 (d, 2 H, J = 8.0, H^3), 7.76 (td, 2 H, J = 7.7, 1.5, H^4), 7.41 (ddd, 2 H, J = 7.4, 4.6, 1.5, H^5), 7.13 (d, 2 H, J = 8.5, H^o), 6.56 (d, 2 H, J = 8.5 Hz, H^m), 4.05 (m, 1 H, CH), 3.63 (br m, 2 H, CH_2) and 3.49 (br s, 2 H, NH_2). ^{13}C NMR ($CDCl_3$): δ 200.9 ($C^{2'}$), 154.2, 148.8 (C^6), 145.0, 136.7 (C^4), 135.4, 128.5, 126.9, 121.8 (C^5), 115.2 (C^3), 44.4 ($C^{4'}$) and 35.4 ($C^{3'}$). IR (Nujol mull): 3395w, 1797s, 1786s, 1584m, 1515m, 1391m, 1278m, 995s, 780m and 771m cm^{-1}. UV/VIS (MeOH): λ_{max}/nm (10^{-3} ε/l mol^{-1} cm^{-1}) 202 (29.0), 233 (21.5) and 269 (8.9).

4′-(4-Anilino)-2,2′:6′,2″-terpyridine (L^1). *Method 1.* 3-(4-Anilino)-1,5-bis(2-pyridyl)pentane-1,5-dione (0.30 g, 0.87 mmol) and ammonium acetate (5.0 g) were heated at reflux in ethanol (100 cm^3) for 4 h. After cooling, water (50 cm^3) was added and the reaction mixture was condensed to 60 cm^3 *in vacuo*. After standing for 1 h the resulting solid was collected and then recrystallised from ethanol, filtered off and washed with diethyl ether to give a light yellow crystalline solid (0.17 g, 60%).

Method 2. Poly(4-aminobenzaldehyde) (9.7 g, 0.08 mol), 2-acetylpyridine (22 cm^3, 0.17 mol), ammonium acetate (75 g, 0.98 mol) and acetamide (100 g, 1.7 mol) were heated in air at reflux for 3 h at 180 °C. The solution was allowed to cool and then NaOH (50 g) in water (200 cm^3) was added and the mixture heated at reflux for 2 h. After cooling the solution was decanted and the oily solid washed with water (3 × 200 cm^3). The sludge was dissolved in the minimum volume of hot concentrated hydrobromic acid, and then the solution allowed to stand at room temperature for 16 h. The dark brown precipitate was filtered off, placed in a beaker with water (300 cm^3) and $NaHCO_3$ added until the solution was basic. The solid was extracted into chloroform, concentrated and purified by flash chromatography (silica, chloroform as the eluent). The brown band (fraction 3) was collected and concentrated to a brown oil that was recrystallised from a chloroform–methanol mixture to give transparent brown crystals (3.1 g, 12%). The other fractions separated by chromatography were not identified. M.p. 256–257 °C (Found: C, 77.72; H, 5.15; N, 17.00. Calc. for $C_{21}H_{16}N_4$: C, 77.78; H, 4.94; N, 17.28%). EI mass spectrum: *m/z* 324 (M^+) and 246 (M^+ − py). ^{1}H NMR ($CDCl_3$): δ 8.73 (br d, 2 H, J = 4.6, H^6), 8.69 (s, 2 H, $H^{3'}$), 8.66 (d, 2 H, J = 8.0, H^3), 7.87 (td, 2 H, J = 7.7, 1.8, H^4), 7.78 (d, 2 H, J = 8.5, H^o), 7.34 (ddd, 2 H, J = 7.7, 4.7, 1.2, H^5), 6.80 (d, 2 H, J = 8.5 Hz, H^m) and 3.90 (br s, NH_2). ^{13}C NMR ($CDCl_3$): δ 157.18, 156.37, 150.62, 149.74

(C^6), 148.16, 137.48 (C^4), 129.05 (C^o), 124.32 (C^5), 122.03 (C^3), 118.47 ($C^{3'}$) and 115.90 (C^m). IR (Nujol mull): 3330w, 1600m, 1585s, 830m, 785s and 728m cm^{-1}. UV/VIS (MeOH): λ_{max}/nm (10^{-3} ε/l mol^{-1} cm^{-1}) 408 (11.3), 326 (16.8), 314 (15.8), 286 (24.4), 234 (22.2) and 204 (35.5).

General method for $[ML^1_2][PF_6]_2$ (M = Co^{II}, Cu^{II}, Mn^{II}, Ni^{II} or Zn^{II}). Compound L^1 (200 mg, 0.62 mmol) was heated to reflux in methanol (200 cm^3) and a solution of the appropriate metal chloride or metal acetate (0.30 mmol) in methanol (20 cm^3) was added dropwise. After 15 min at reflux, a methanolic solution of ammonium hexafluorophosphate was added and the solution allowed to cool whereupon a microcrystalline precipitate of the appropriate hexafluorophosphate salt was obtained. The salt was recrystallised from methanol, filtered off and washed with diethyl ether. Yields were in the range 60–85%.

$[CoL^1_2][PF_6]_2$. A maroon microcrystalline solid (Found: C, 48.31; H, 3.36; N, 10.45. Calc. for $C_{42}H_{32}CoF_{12}N_8P_2{\cdot}2H_2O$: C, 48.79; H, 3.49; N, 10.84%). ES mass spectrum: *m/z* 353 (M^{2+}) and 852 ($[M + PF_6]^+$). UV/VIS (acetone): λ_{max}/nm (ε/l mol^{-1} cm^{-1}) 716 (sh) (200).

$[CuL^1_2][PF_6]_2$. A green microcrystalline solid (Found: C, 50.11; H, 3.47; N, 11.02. Calc. for $C_{42}H_{32}CuF_{12}N_8P_2$: C, 50.32; H, 3.20; N, 11.18%). ES mass spectrum: *m/z* 356 (M^{2+}) and 856 ($[M + PF_6]^+$). UV/VIS (acetone): λ_{max}/nm (ε/l mol^{-1} cm^{-1}) 685 (100).

$[MnL^1_2][PF_6]_2$. A yellow microcrystalline solid (Found: C, 50.55; H, 3.43; N, 11.00. Calc. for $C_{42}H_{32}F_{12}MnN_8P_2$: C, 50.76; H, 3.22; N, 11.28%). ES mass spectrum: *m/z* 352 (M^{2+}) and 851 ($[M + PF_6]^+$). IR (Nujol mull): 3395w, 1605m, 1017m, 850s, 840s, 821s, 792m and 784m cm^{-1}.

$[NiL^1_2][PF_6]_2$. A yellow microcrystalline solid (Found: C, 48.72; H, 3.40; N, 10.68. Calc. for $C_{42}H_{32}F_{12}N_8NiP_2{\cdot}2H_2O$: C, 48.80; H, 3.49; N, 10.84%). ES mass spectrum: *m/z* 353 (M^{2+}) and 851 ($[M + PF_6]^+$). IR (Nujol mull): 3400w, 1603s, 1576m, 1554m, 1527m, 1469m, 1190m, 1028m, 1015m, 843s and 792m cm^{-1}. UV/VIS (acetone): λ_{max}/nm (ε/l mol^{-1} cm^{-1}) 804 (130).

$[ZnL^1_2][PF_6]_2$. A light yellow microcrystalline solid (Found: C, 49.96; H, 3.43; N, 10.85. Calc. for $C_{42}H_{32}F_{12}N_8P_2Zn$: C, 49.91; H, 3.17; N, 11.09%). ES mass spectrum: *m/z* 356 (M^{2+}) and 857 ($[M + PF_6]^+$). ^{13}C NMR [$(CD_3)_2CO$]: δ 157.42, 153.58, 150.90, 149.84, 149.22, 142.37, 128.66, 124.31, 123.80, 119.89 and 115.75. IR (Nujol mull): 3395w, 1598s, 1520w, 1190w, 1020m, 1011m, 832s, 790m and 783m cm^{-1}.

$[FeL^1_2][BF_4]_2$. A solution of $[Fe(H_2O)_6][BF_4]_2$ (186 mg, 0.55 mmol) in methanol (10 cm^3) was added dropwise to a methanolic solution (150 cm^3) of L^1 (380 mg, 1.17 mmol) at reflux. The mixture was heated at reflux for 10 min and allowed to cool. The resulting precipitate was filtered off and then recrystallised from methanol as a purple microcrystalline solid (390 mg, 80%) (Found: C, 55.50; H, 3.97; N, 12.05. Calc. for $C_{42}H_{32}B_2F_8FeN_8{\cdot}2H_2O$: C, 55.18; H, 3.94; N, 12.26%). ES mass spectrum: *m/z* 352 (M^{2+}) and 791 ($[M + BF_4]^+$). ^{13}C NMR [$(CD_3)_2CO$]: δ 161.40, 160.00, 154.46, 153.21, 151.87, 139.90, 130.17, 128.57, 124.94, 124.53, 120.52 and 115.89. IR (Nujol mull): 3490w, 1600s, 1526w, 1415m, 1190m, 1056s, 835w and 788m cm^{-1}.

$[RhL^1_2][PF_6]_3$. Compound L^1 (200 mg, 0.62 mmol) was dissolved in hot methanol (200 cm^3), $RhCl_3{\cdot}3H_2O$ (80 mg, 0.31 mmol) in distilled water (10 cm^3) was added dropwise and the resulting solution heated at reflux for 30 min. The solution was condensed *in vacuo* to 50 cm^3 and the product was precipitated by the addition of an excess of aqueous $[NH_4][PF_6]$. After filtering the solid, it was recrystallised from acetonitrile–methanol to afford an orange-brown microcrystalline solid (238 mg, 62%) (Found: C, 43.76; H, 3.43; N, 10.85. Calc. for $C_{42}H_{32}F_{18}N_8P_3Rh{\cdot}2MeCN$: C, 43.54; H, 3.00; N, 11.04%). ES mass spectrum: *m/z* 251 (M^{3+}), 448 ($[M + PF_6]^{2+}$) and 1042 ($[M + 2PF_6]^+$). ^{13}C NMR [$(CD_3)_2CO$]: δ 159.32, 157.13, 154.87, 154.68, 154.22, 143.92, 131.20, 128.40, 122.85, 116.16 and 115.92. IR (Nujol mull): 3395w, 1630w, 1590s, 1528w, 1420w, 1310w, 1295w, 1268w, 1243m, 1194m, 1165w, 1100w, 1044w, 1030, 966w, 839s, 781m, 748w and 719w cm^{-1}.

$[RuL^1_2][PF_6]_2$. Compound L^1 (106 mg, 0.33 mmol) was dissolved in ethanol (120 cm^3) at reflux. The complex $[Ru(dmso)_4Cl_2]$ (79 mg, 0.16 mmol) in distilled water (50 cm^3) was slowly added and the resulting solution heated at reflux for 30 min. The solvent was removed *in vacuo* and the residue dissolved in the minimum volume of methanol and purified by gel permeation chromatography (Sephadex LH20, methanol eluent). The central bright red band was collected and the product precipitated by the addition of an excess of aqueous $[NH_4][PF_6]$ to afford a red microcrystalline solid (92 mg, 55%) (Found: C, 47.07; H, 3.56; N, 10.77. Calc. for $C_{42}H_{32}F_{12}N_8P_2Ru{\cdot}2H_2O$: C, 46.85; H, 3.35; N, 10.41%). ES mass spectrum: *m/z* 375 (M^{2+}) and 895 ($[M + PF_6]^+$). ^{13}C NMR [$(CD_3)_2CO$]: δ 159.5, 156.1, 153.1 (C^6), 152.1, 149.2, 138.6 (C^4), 129.3 (C^o), 128.1 (C^5), 125.1 (C^3), 123.1, 119.9 ($C^{3'}$) and 115.3 (C^m). IR (Nujol mull): 3400w, 1600m, 1520w, 1404w, 1184w, 842s, 833s and 784w cm^{-1}.

$[Ru(terpy)L^1][PF_6]_2$. The complex $[Ru(terpy)Cl_3]$ (272 mg, 0.62 mmol) was reduced by triethylamine in the presence of L^1 (200 mg, 0.62 mmol) in ethanol (200 cm^3) and water (10 cm^3) heated at reflux for 18 h. The solvent was removed *in vacuo* and the residue dissolved in the minimum volume of acetonitrile and purified by flash chromatography [silica, acetonitrile–water–saturated KNO_3 (aq) 20:2:1 eluent]. The bright red second band was collected and precipitated by the addition of an excess of aqueous $[NH_4][PF_6]$ to afford a red crystalline solid (320 mg, 55%) (Found: C, 44.86; H, 3.40; N, 9.95%. Calc. for $C_{36}H_{27}F_{12}N_7Ru{\cdot}H_2O$: C, 44.69; H, 3.00; N, 10.14%). ES mass spectrum: *m/z* 329 (M^{2+}) and 804 ($[M + PF_6]^+$). ^{13}C NMR [$(CD_3)_2CO$]: δ 160.0, 159.7, 157.0, 153.9, 153.7, 150.2, 139.4, 137.0, 130.0, 129.0, 128.8, 125.8, 125.1, 120.6 and 115.9. IR (Nujol mull): 3300w, 1598m, 1408w, 1190w, 838s and 765m cm^{-1}.

4′-(4-Phthalimidophenyl)-2,2′:6′,2″-terpyridine (L^2). *Method 1.* Compound L^1 (129 mg, 0.40 mmol) and phthalic anhydride (59 mg, 0.40 mmol) were stirred at room temperature in dma (10 cm^3) for 20 h. Acetic anhydride (2 cm^3) was added and the solution heated at 80 °C for 5 h. After cooling the product was precipitated by the addition of water (100 cm^3) and filtered off. The solid was then recrystallised from ethanol to afford dark yellow needles (130 mg, 72%).

Method 2. Compound L^1 (120 mg, 0.38 mmol) and phthalic anhydride (57 mg, 0.38 mmol) were dissolved in nmp (20 cm^3) and heated at 160 °C for 16 h. Dropwise addition to a stirring water solution (200 cm^3) resulted in the formation of a precipitate which was filtered off and recrystallised from ethanol to afford dark yellow needles (125 mg, 74%). M.p. 254–256 °C (Found: C, 76.19; H, 4.37; N, 12.28. Calc. for $C_{29}H_{18}N_4O_2$: C, 76.65; H, 3.96; N, 12.33%). EI mass spectrum: *m/z* 454 (M^+) and 376 ($M - py)^+$. ^{1}H NMR ($CDCl_3$): δ 8.78 (s, 2 H, $H^{3'}$), 8.74 (d, 2 H, J = 4.6, H^6), 8.68 (d, 2 H, J = 8.0, H^3), 8.06 (d, 2 H, J = 8.7, H^o), 7.99 (m, 2 H, H^A), 7.89 (td, 2 H, J = 7.7, 1.8, H^4), 7.82 (m, 2 H, H^B), 7.65 (d, 2 H, J = 8.7, H^m) and 7.36 (ddd, 2 H, J = 7.7, 5.2, 1.7 Hz, H^5). ^{13}C NMR ($CDCl_3$): δ 167.12, 156.14, 156.08, 149.29, 149.16, 138.16, 136.84, 134.49, 132.45, 131.74, 128.02, 126.76, 123.84, 123.82, 121.34 and 118.87. IR (Nujol mull): 1774w, 1757w, 1740w, 1718s, 1602w, 1582m, 1564w, 1536w, 1510m, 1412w, 1261w, 1220w, 1159w, 1139w, 1114w, 1072w, 1037w, 1012w, 985w, 900w, 889w, 879w, 843w, 829m, 814w, 804w, 790w and 783m cm^{-1}.

4′-(4-Benzamidophenyl)-2,2′:6′,2″-terpyridine (L^3). Compound L^1 (125 mg, 0.39 mmol) was dissolved in a mixture of nmp (8 cm^3) and pyridine (2 cm^3). An excess of benzoyl chlor-

ide (3 drops) was added and the solution stirred at room temperature for 18 h. The product was precipitated by dropwise addition to a stirring solution of diethyl ether (150 cm^3), filtered and then recrystallised from methanol to give yellow feathery needles (151 mg, 92%), m.p. 220–223 °C (Found: C, 66.94; H, 5.18; N, 10.77. Calc. for $C_{29}H_{18}N_4O_2·4H_2O$: C, 67.20; H, 5.60; N, 11.20%). EI mass spectrum: 428 (M^+), 323 {[M − $C_6H_5C(O)]^+$} and 105 [$C_6H_5C(O)$]. ^{1}H NMR [$(CD_3)_2SO$]: δ 10.56 (br s, 1 H, NH), 8.99 (d, 2 H, J = 7.7, H^6), 8.94 (d, 2 H, J = 8.0, H^3), 8.93 (s, 2 H, $H^{3'}$), 8.38 (br t, 2 H, J = 6.7, H^4), 8.15 (m, 4 H, H^o and H^m), 8.06 (d, 2 H, H^A), 7.83 (br t, 2 H, J = 5.6, H^5), 7.67 (t, 1 H, J = 7.2, H^C) and 7.61 (t, 2 H, J = 6.8 Hz, H^B). ^{13}C NMR [$(CD_3)_2SO$]: δ 166.07, 153.13, 152.16, 150.08, 147.28, 141.29, 141.20, 134.91, 132.08, 131.51, 128.71, 128.01, 127.87, 126.09, 122.99, 120.94 and 119.38. IR (Nujol mull): 3350m (br), 1664m, 1594s, 1397w, 1374w, 1325w, 1295w, 1260 (sh) w, 1237w, 1190w, 1055w, 1018w, 990w, 950w, 888w, 836w, 781m, 705m and 655w cm^{-1}.

[FeL$^2_2$][BF$_4$]$_2$. The complex [FeL$^1_2$][BF$_4$]$_2$ (114 mg, 0.13 mmol) and phthalic anhydride (42 mg, 0.27 mmol) were dissolved in dma (10 cm^3) and stirred at room temperature for 18 h. Acetic anhydride (4 cm^3) and pyridine (2 cm^3) were added and the solution heated to 80 °C for 5 h. After cooling it was precipitated by dropwise addition to a stirring solution of diethyl ether (200 cm^3). The solid was filtered off, dissolved in the minimum volume of acetonitrile and purified by flash chromatography [silica, acetonitrile–water–saturated KNO_3 (aq) 20:2:1 eluent]. The initial light purple band eluted was identified by ^{1}H NMR spectroscopy as a 1:3 mixture of unreacted [FeL$^1_2$]$^{2+}$ and the acetamidophenylterpyridyl complex, [FeL$^4_2$]$^{2+}$. The broad second purple band was collected and the product precipitated with the addition of an excess of aqueous [NH_4][BF_4] to afford a purple powder (85 mg, 58%) (Found: C, 61.56; H, 3.88; N, 11.49. Calc. for $C_{58}H_{36}B_2F_8FeN_8O_4·2CH_3CN$: C, 61.01; H, 3.44; N, 11.48%). ES mass spectrum: m/z 482 (M^{2+}). ^{13}C NMR [$(CD_3)_2SO$]: δ 167.10, 160.14, 158.02, 156.02, 148.51, 138.98, 135.57, 134.17, 131.77, 128.49, 128.10, 127.79, 124.26, 123.75 and 121.45. IR (Nujol mull): 1720m, 1596w, 1520w, 1415w, 1191w, 1060s, 842w and 786m cm^{-1}.

[FeL$^3_2$][BF$_4$]$_2$. The complex [FeL$^1_2$][BF$_4$]$_2$ (97 mg, 0.12 mmol) was dissolved in acetonitrile (50 cm^3), pyridine (4 cm^3) and an excess of benzoyl chloride (5 drops) were added and the solution heated at reflux for 16 h. Over this period a purple solid precipitated and after cooling it was filtered off and washed with water and diethyl ether. The solid was recrystallised from methanol to afford a purple powder (100 mg, 80%) (Found: C, 57.71; H, 4.15; N, 9.70. Calc. for $C_{56}H_{40}B_2F_8FeN_8O_2·4H_2O$: C, 58.06; H, 4.15; N, 9.68%). ES mass spectrum: m/z 456 (M^{2+}) and 1000 ([M + BF_4]$^+$). ^{13}C NMR [$(CD_3)_2SO$]: δ 166.57, 160.25, 158.35, 153.16, 149.01, 141.87, 139.23, 134.97, 132.50, 131.22, 129.08, 128.80, 128.22, 128.03, 124.49, 121.10 and 120.90. IR (Nujol mull): 3380w, 1665m, 1590m, 1517m, 1190w, 1050w and 832w cm^{-1}.

[FeL$^4_2$][BF$_4$]$_2$. *Method 1.* The complex [FeL$^1_2$][BF$_4$]$_2$ (60 mg, 0.07 mmol) and an excess of acetyl chloride were heated at reflux in acetonitrile (50 cm^3) and pyridine (2 cm^3) for 6 h. The purple solid that precipitated from the solution during this period was filtered off and recrystallised from methanol to give a purple microcrystalline solid (48 mg, 73%).

Method 2. The complex [FeL$^1_2$][BF$_4$]$_2$ (35 mg, 0.04 mmol), acetic anhydride (4 cm^3) and pyridine (2 cm^3) were stirred in dma (10 cm^3) at room temperature for 1 h and then heated at 80 °C for 3 h. Dropwise addition of the solution to diethyl ether (200 cm^3) resulted in a purple precipitate (the ^{1}H NMR spectrum showed quantitative conversion into the acetamide complex) which was filtered off and then dissolved in the minimum volume of acetonitrile. Purification by flash chromatography [silica, acetonitrile–water–saturated KNO_3 (aq) 20:2:1 eluent] gave a broad purple band which was collected and precipitated with the addition of an excess of [NH_4][BF_4] to give a purple microcrystalline solid (23 mg, 57%) (Found: C, 54.11; H, 4.56; N, 10.72. Calc. for $C_{46}H_{36}B_2F_8FeN_8O_2·3H_2O$: C, 54.38; H, 4.14; N, 11.03%). ES mass spectrum: m/z 394 (M^{2+}) and 877 ([M + BF_4]$^+$). ^{13}C NMR [$(CD_3)_2SO$]: δ 169.08, 159.93, 158.08, 152.95, 148.68, 141.90, 138.85, 130.17, 128.55, 127.69, 124.12, 120.48, 119.42 and 24.39. ^{1}H NMR [$(CD_3)_2CO$]: δ 9.55 (s, 2 H, $H^{3'}$), 9.52 (br s, NH), 8.97 (d, 2 H, J = 7.9, H^3), 8.38 (d, 2 H, J = 8.7, H^o), 8.02 (m, 4 H, H^m and H^4), 7.53 (d, 2 H, J = 5.1, H^6), 7.21 (t, 2 H, J = 6.7 Hz, H^5) and 2.78 (s, 3 H, CH_3). IR (Nujol mull): 3400w, 1692m, 1596m, 1521m, 1412m, 1320w, 1304w, 1248w, 1190w, 1060s, 834w and 790m cm^{-1}.

[Ru(terpy)L^2][PF$_6$]$_2$. The complex [Ru(terpy)L^1][PF$_6$]$_2$ (60 mg, 0.06 mmol) and phthalic anhydride (20 mg, 0.13 mmol) were dissolved in nmp (15 cm^3) and stirred at 145 °C for 20 h. After cooling it was precipitated by dropwise addition to a stirring solution of diethyl ether (200 cm^3). The solid was filtered off, dissolved in the minimum volume of acetonitrile and purified by flash chromatography [silica, acetonitrile–water–saturated KNO_3 (aq) 20:2:1 eluent]. The first and second bands were identified by ^{1}H NMR spectroscopy as unchanged [Ru(terpy)L^1]$^{2+}$ (9% yield) and the acetamido complex [Ru(terpy)L^4]$^{2+}$ (8% yield) respectively. The third dark red band was collected and the product precipitated by the addition of an excess of aqueous [NH_4][PF_6] and recrystallised from aqueous acetonitrile to afford a red powder (38 mg, 55%) (Found: C, 48.59; H, 3.06; N, 9.10. Calc. for $C_{44}H_{29}F_{12}N_7O_2P_2Ru·0.5H_2O$: C, 48.55; H, 2.94; N, 9.01%). ES mass spectrum: m/z 394 (M^{2+}) and 934 ([M + PF_6]$^+$). ^{13}C NMR [$(CD_3)_2CO$]: δ 168.19, 159.7, 159.6, 157.1, 156.8, 153.9, 153.8, 148.9, 139.53, 139.48, 137.4, 136.1, 133.3, 129.4, 129.02, 129.00, 126.0, 125.8, 125.2, 124.7 and 122.9. IR (Nujol mull): 1780s, 1760s, 1742s, 1719m, 1517w, 1410w, 1220w, 1158w, 1130w, 1070w and 836s cm^{-1}.

[Ru(terpy)L^3][PF$_6$]$_2$. The complex [Ru(terpy)L^1][PF$_6$]$_2$ (53 mg, 0.06 mmol) was dissolved in freshly distilled acetonitrile (35 cm^3), benzoyl chloride (4 drops) and pyridine (2 cm^3) were added and the solution heated at reflux for 6 h. During this period a red solid precipitated. After cooling this solid was filtered off and washed with diethyl ether until all traces of pyridine were removed. The product was recrystallised from methanol to give a red microcrystalline solid which was filtered off and washed with diethyl ether. A second portion of the product was obtained from the initial filtrate by condensing the solution *in vacuo*, dissolving the residue in the minimum volume of acetonitrile and purified by flash chromatography [silica, acetonitrile–water–saturated KNO_3 (aq) 20:2:1 eluent]. The bright red second band was collected and the product precipitated by the addition of an excess of aqueous [NH_4][PF_6] to afford a red powder (40 mg, 68%) (Found: C, 49.16; H, 3.32; N, 9.04. Calc. for $C_{43}H_{31}F_{12}N_7OP_2Ru$: C, 49.02; H, 2.94; N, 9.31%). ES mass spectrum: m/z 382 (M^{2+}) and 907 ([M + PF_6]$^+$). ^{13}C NMR [$(CD_3)_2SO$]: δ 166.18, 158.24, 157.94, 155.15, 155.01, 152.34, 152.24, 149.81, 146.70, 141.59, 138.27, 134.84, 132.11, 130.91, 128.71, 128.39, 127.99, 125.03, 124.73, 124.19, 120.74 and 120.64. IR (Nujol mull): 3360w (br) 1658m, 1595m, 1518w, 1238w, 1190w, 1024w, 882w, 840m, 778w and 750m cm^{-1}.

[Ru(terpy)L^4][PF$_6$]$_2$. *Method 1.* The complex [Ru(terpy)-L^1][PF$_6$]$_2$ (100 mg, 0.1 mmol) was dissolved in dma (10 cm^3) and stirred with acetic anhydride (4 cm^3) and pyridine (2 cm^3), the solution heated to 80 °C for 3 h and then stirred at room temperature for 16 h. The products were precipitated by dropwise addition to a stirring solution of diethyl ether (200 cm^3) and filtered off. The solid was dissolved in the minimum volume of acetonitrile and purified by flash chromatography [silica,

acetonitrile–water–saturated KNO_3 (aq) 20:2:1 eluent]. The initial red band was collected and the product precipitated by the addition of an excess of aqueous $[NH_4][PF_6]$ to afford a red microcrystalline solid (55 mg, 50%) (Found: C, 44.50; H, 3.46; N, 9.45. Calc. for $C_{38}H_{29}F_{12}N_7OP_2Ru\cdot 2H_2O$: C, 44.44; H, 3.22; N, 9.55%). ES mass spectrum: *m*/*z* 357 (M^{2+}) and 860 ($[M + PF_6]^+$). ^{13}C NMR [$(CD_3)_2CO$]: δ 169.83, 159.83, 159.64, 158.92, 153.89, 153.82, 149.23, 143.20, 139.48, 137.29, 132.04, 129.50, 129.02, 128.96, 125.95, 125.78, 125.16, 122.01, 120.82, 120.74 and 24.78. IR (Nujol mull): 3400w, 1676m, 1603m, 1592m, 1520m, 1190w, 1159w, 1025w, 840s and 765m cm^{-1}.

***N*,*N*′-Bis[4-(2,2′:6′,2″-terpyridin-4′-yl)phenyl]pyromellitimide (L^5).** Pyromellitic dianhydride (74 mg, 0.34 mmol) was slowly added to L^1 (220 mg, 0.68 mmol) dissolved in dma (8 cm^3) and stirred at room temperature for 18 h. At this point the bis(amic acid), aa, can be precipitated by addition of diethyl ether, m.p. >350 °C (Found: C, 66.70; H, 4.43; N, 11.36. Calc. for $C_{52}H_{34}N_8O_6\cdot 4H_2O$: C, 66.52; H, 4.47; N, 11.94%). ^{1}H NMR [$(CD_3)_2SO$]: δ 10.85 (s, 2 H, OH), 8.78 (br d, 4 H, H^6), 8.75 (s, 4 H, H$^{3'}$), 8.69 (d, 4 H, H^3), 8.00 (m, 14 H, H^o, H^m, H^4 and H^p) and 7.54 (br t, 4 H, H^5). If instead a mixture of acetic anhydride (8 cm^3) and pyridine (4 cm^3) was added and the solution stirred, the product precipitated. After 1 h the precipitated solid was filtered off, boiled in methanol and then filtered whilst hot, washed with diethyl ether and dried to give a dull yellow powder (258 mg, 91%), m.p. >350 °C (Found: C, 70.88; H, 4.02; N, 12.49. Calc. for $C_{52}H_{30}N_8O_4\cdot 3H_2O$: C, 70.59; H, 4.07; N, 12.67%). EI mass spectrum: *m*/*z* 830 (M^+). ^{1}H NMR (CF_3CO_2D): δ 9.23 (d, 4 H, *J* = 5.4, H^6), 9.03 (d, 4 H, *J* = 8.3, H^3), 8.93 (m, 8 H, H^4 and H$^{3'}$), 8.77 (s, 2 H, H^p), 8.32 (t, 4 H, *J* = 7.0, H^5), 8.18 (d, 4 H, *J* = 8.3, H^o) and 7.88 (d, 4 H, *J* = 8.2 Hz, H^m). ^{13}C NMR (CF_3CO_2D): δ 190.63, 153.65, 141.14, 135.21, 134.35, 133.59, 129.34, 124.21, 123.24, 119.68, 115.37, 115.05, 114.83, 111.70 and 110.30. IR (Nujol mull): 1778w, 1740s, 1590m, 1570w, 1548w, 1520m, 1198w, 1038w, 810m, 785m and 730m cm^{-1}.

***N*,*N*′-Bis[4-(2,2′:6′,2″-terpyridin-4′-yl)phenyl]terephthalamide (L^6).** Terephthaloyl chloride was added to L^1 (300 mg, 0.93 mmol) dissolved in dma (25 ml) and pyridine (8 cm^3) with stirring at room temperature. A light yellow solid began to precipitate almost immediately. The mixture was stirred for 2 h and then the solid was filtered off and washed with diethyl ether to give a light yellow powder. A second portion of the product was obtained by precipitation upon addition of the filtrate to methanol (150 cm^3). This solid was filtered off, washed with methanol and diethyl ether to afford a light yellow powder (255 mg, 70%), m.p. >350 °C (Found: C, 73.18; H, 5.39; N, 14.14. Calc. for $C_{50}H_{38}N_8O_2\cdot 1.5H_2O$: C, 73.38; H, 5.22; N, 14.27%). ^{1}H NMR (CF_3CO_2D): δ 9.21 (d, 4 H, *J* = 5.9, H^6), 9.03 (d, 4 H, *J* = 8.5, H^3), 8.91 (m, 8 H, H^4 and H$^{3'}$), 8.30 (t, 4 H, *J* = 6.5, H^5), 8.28 (s, 4 H, H^p), 8.09 (d, 4 H, *J* = 9.0, H^o) and 8.03 (d, 4 H, *J* = 8.6 Hz, H^m). ^{13}C NMR (CF_3CO_2D): δ 184.25, 152.88, 137.73, 131.48, 130.40, 129.97, 125.49, 122.10, 116.17, 111.48, 107.92, 106.63 and 106.14. IR (Nujol mull): 3250w, 1670m, 1598s, 1582w, 1516m, 1412w, 1323m, 1298w, 1257m, 1185w, 1104w, 1070w, 1035w, 1010w, 984w, 878w, 863w, 828m and 782m cm^{-1}.

***N*,*N*′-Bis[4-(2,2′:6′,2″-terpyridin-4′-yl)phenyl]adipamide (L^7).** Adipoyl chloride (47 mg, 0.25 mmol) was added to L^1 (166 mg, 0.51 mmol) dissolved in dma (15 cm^3) and pyridine (4 cm^3) at 120 °C and the solution was stirred for 2 h. After cooling the resulting precipitate was filtered off and washed with methanol and diethyl ether to give a cream flaky solid (143 mg, 73%), m.p. >350 °C (Found: C, 69.52; H, 5.48; N, 13.70. Calc. for $C_{48}H_{38}N_8O_2\cdot 4H_2O$: C, 69.40; H, 5.54; N, 13.49%). EI mass spectrum: *m*/*z* 766 (M^+). ^{1}H NMR (CF_3CO_2D): δ 9.19 (d, 4 H, *J* = 5.6, H^6), 9.00 (d, 4 H, *J* = 7.7, H^3), 8.89 (t, 4 H, *J* = 8.2, H^4), 8.86 (s, 4 H, H$^{3'}$), 8.29 (t, 4 H, *J* = 6.7, H^5), 8.01 (d, 4 H, *J* = 8.2, H^o), 7.87 (d, 4 H, *J* = 8.7 Hz, H^m), 2.85 (br s, 4 H, CH_2) and 2.11 (br s, 4 H, CH_2). ^{13}C NMR (CF_3CO_2D): δ 163.89, 141.35, 135.13, 134.02, 133.62, 129.12, 125.15, 119.92, 114.92, 114.85, 111.58, 110.17, 109.82, 22.51 and 11.54. IR (Nujol mull): 3320w (br), 1655m, 1590m, 1575s, 1558w, 1510s, 1405w, 1305w, 1290w, 1250w, 1218w, 1178w, 1105w, 1062w, 1026w, 978w, 940w, 875w, 822m, 778s and 735w cm^{-1}.

[(terpy)RuL^{5}Ru(terpy)][PF$_6$]$_4$. *Method* (*a*). (*i*) The complex [Ru(terpy)Cl$_3$] (163 mg, 0.37 mmol) and $AgSbF_6$ (381 mg, 1.11 mmol) were heated at reflux for 3 h in acetone (60 cm^3). The reaction mixture was filtered to remove the precipitated AgCl and the filtrate added to dmf (30 cm^3). The acetone was removed *in vacuo* and the dmf solution added to a solution of L^5 (160 mg, 0.18 mmol) in dmf (350 cm^3) and heated at reflux under N_2 for 5 h. The reaction mixture was filtered to remove unreacted L^5 and then dmf (300 cm^3) was removed by distillation and the products precipitated by the addition of an excess of $[NH_4][PF_6]$ in water (50 cm^3). The solid was filtered off, dissolved in acetonitrile and purified by flash chromatography [silica, acetonitrile–water–saturated KNO_3 (aq) 20:2:1 eluent]. The first fraction was identified as [Ru(terpy)$_2$]$^{2+}$ (15% yield), while the second band was a mixture of complexes which were not separated. The broad slow-moving third band was collected and precipitated with an excess of aqueous $[NH_4][PF_6]$. The solid was filtered off and recrystallised from aqueous acetonitrile to give a red microcrystalline solid (123 mg, 32%).

(*ii*) The complex [Ru(terpy)Cl$_3$] (100 mg, 0.23 mmol) and L^5 (92 mg, 0.11 mmol) in ethane-1,2-diol (20 cm^3) were heated at reflux for 20 min. The products were precipitated by the addition of an excess of $[NH_4][PF_6]$ in water (50 cm^3). The solid was filtered off, dissolved in acetonitrile and purified by flash chromatography [silica, acetonitrile–water–saturated KNO_3 (aq) 20:2:1 eluent]. The first fraction was identified as [Ru(terpy)$_2$]$^{2+}$ (8% yield), while the second band was a mixture of complexes which were not separated. The broad slow-moving third band was collected and precipitated with an excess of aqueous $[NH_4][PF_6]$. The solid was filtered off and recrystallised from aqueous acetonitrile to give a red microcrystalline solid (155 mg, 44%).

Method (*b*). The complex [Ru(terpy)L^1][PF$_6$]$_2$ (165 mg, 0.16 mmol) and pyromellitic dianhydride (19 mg, 0.08 mmol) were stirred at room temperature for 18 h in dma (10 cm^3). A mixture of pyridine (2 cm^3) and acetic anhydride (4 cm^3) was added and the solution heated to 80 °C for 3 h. The products were precipitated by dropwise addition to diethyl ether (250 cm^3) and the solid filtered off and dissolved in acetonitrile. Purification by flash chromatography [silica, acetonitrile–water–saturated KNO_3 (aq) 20:2:1 eluent] led to three bands separating on the column. The first band was identified (^{1}H NMR and mass spectroscopies) as the acetamidophenylterpyridine complex, [Ru(terpy)L^4]$^{2+}$ (24% yield) and the second band contained a mixture of complexes which were not separated. The third band was collected and precipitated with an excess of aqueous $[NH_4][PF_6]$. The solid was filtered off and recrystallised from aqueous acetonitrile to give a red microcrystalline solid (72 mg, 40%) (Found: C, 47.13; H, 3.05; N, 8.50. Calc. for $C_{82}H_{52}F_{24}N_{14}O_4P_4Ru_2$: C, 47.37; H, 2.50; N, 9.44%). ES mass spectrum: *m*/*z* 375 (M^{4+}), 548 ($[M + PF_6]^{3+}$) and 896 ($[M + 2PF_6]^{2+}$). ^{13}C NMR [$(CD_3)_2SO$]: δ 165.63, 158.19, 157.98, 155.36, 154.96, 152.40, 146.25, 138.36, 137.47, 136.17, 133.50, 129.08, 128.54, 128.40, 127.95, 125.47, 125.01, 124.77, 124.23, 121.56 and 118.38. IR (Nujol mull): 1775w, 1720m, 1600w, 1510w, 1404w, 1282w, 1240w, 1198w, 1025w and 835s cm^{-1}.

[(terpy)RuL^{6}Ru(terpy)][PF$_6$]$_4$. *Method* (*a*). The complex [Ru(terpy)Cl$_3$] (170 mg, 0.39 mmol) and $AgSbF_6$ (398 mg, 1.16 mmol) were heated at reflux for 3 h in acetone (60 cm^3). The

reaction mixture was filtered to remove the precipitated AgCl and added to dmf (30 cm^3). The acetone was removed *in vacuo* and the dmf solution added to a solution of L^6 (150 mg, 0.19 mmol) in dmf (400 cm^3) and heated at reflux for 5 h. The dmf (250 cm^3) was removed by distillation and the products precipitated by the addition of an excess of $[NH_4][PF_6]$ in water (100 cm^3). The solid was filtered off, dissolved in acetonitrile and purified by flash chromatography [silica, acetonitrile–water–saturated KNO_3 (aq) 20:2:1 eluent]. The broad slow-moving third band was collected and precipitated with an excess of aqueous $[NH_4][PF_6]$. The solid was filtered off and recrystallised from aqueous acetonitrile to give a red microcrystalline solid (175 mg, 48%).

Method (*b*). The complex $[Ru(terpy)L^1][PF_6]_2$ (101 mg, 0.11 mmol) and terephthaloyl chloride (21.6 mg, 0.05 mmol) were heated at 180 °C for 16 h in a dma (10 cm^3)–pyridine (5 cm^3) mixture. After cooling the mixture was precipitated by dropwise addition to diethyl ether (250 cm^3) and the solid filtered off and dissolved in acetonitrile. The first and second bands were identified as $[Ru(terpy)L^1]^{2+}$ (3% yield) and $[Ru(terpy)_2]^{2+}$ (10% yield), respectively. Purification by flash chromatography [silica, acetonitrile–water–saturated KNO_3 (aq) 20:2:1 eluent]. The third band was collected and precipitated with an excess of aqueous $[NH_4][PF_4]$. The solid was filtered off and recrystallised from aqueous acetonitrile to give a red microcrystalline solid (49 mg, 44%) (Found: C, 47.70; H, 2.93; N, 9.95. Calc. for $C_{80}H_{56}F_{24}N_{14}O_2P_4Ru_2\cdot CH_3CN$: C, 47.60; H, 2.85; N, 10.15%). ES mass spectrum: *m*/*z* 362 (M^{4+}), 531 ($[M + PF_6]^{3+}$) and 869 ($[M + 2PF_6]^{2+}$). ^{13}C NMR [$(CD_3)_2SO$]: δ 165.39, 158.25, 157.98, 155.20, 155.01, 152.37, 146.58, 141.35, 138.28, 137.68, 136.01, 131.24, 128.36, 128.19, 127.95, 124.99, 124.74, 124.20, 120.86 and 120.67. IR (Nujol mull): 3420w, 1648w, 1595m, 1520w, 1329w, 1284w, 1180m, 1080m, 846m, 836s, 827s, 783m and 768m cm^{-1}.

[(terpy)RuL^{7}Ru(terpy)][PF$_6$]$_4$. *Method* (*a*). The complex $[Ru(terpy)Cl_3]$ (88 mg, 0.20 mmol) and L^7 (76 mg, 0.10 mmol) were heated at reflux for 15 min in ethane-1,2-diol (15 cm^3). After cooling the products were precipitated by the addition of an excess of $[NH_4][PF_6]$ in water (20 cm^3). The solid was filtered off, dissolved in acetonitrile and purified by flash chromatography [silica, acetonitrile–water–saturated KNO_3 (aq) 20:2:1 eluent]. The broad slow-moving third band was collected and precipitated with an excess of aqueous $[NH_4][PF_6]$. The solid was filtered off and recrystallised from aqueous acetonitrile to give a red microcrystalline solid (82 mg, 41%).

Method (*b*). The complex $[Ru(terpy)L^1][PF_6]_2$ (250 mg, 0.26 mmol) and adipoyl chloride (24 mg, 0.13 mmol) were heated at reflux for 20 h in dmf (15 cm^3) and pyridine (2 cm^3). After cooling the mixture was precipitated by dropwise addition to diethyl ether (250 cm^3) and the solid filtered off and dissolved in acetonitrile. Purification by flash chromatography [silica, acetonitrile–water–saturated KNO_3 (aq) 20:2:1 eluent]. The third band was collected (the first, second and fourth fractions were collected and identified, selected data are given below) and precipitated with an excess of aqueous $[NH_4][PF_6]$. The solid was filtered off and recrystallised from aqueous acetonitrile to give a red microcrystalline solid (78 mg, 30%) (Found: C, 44.08; H, 3.56; N, 9.00. Calc. for $C_{78}H_{68}F_{24}N_{14}O_2P_4Ru_2\cdot 6H_2O$: C, 44.27; H, 3.41; N, 9.27%). ES mass spectrum: *m*/*z* 357 (M^{4+}), 523 ($[M + PF_6]^{3+}$) and 859 ($[M + 2PF_6]^{2+}$). ^{13}C NMR [$(CD_3)_2SO$]: δ 171.83, 158.22, 157.98, 155.12, 155.01, 152.32, 146.66, 141.64, 138.22, 135.96, 130.32, 128.41, 127.90, 124.93, 124.72, 124.18, 120.48, 119.49, 36.60 and 24.98. IR (Nujol mull): 3400w (br), 1665w, 1600m, 1520w, 1505w, 1402w, 1300w, 1026w and 839s cm^{-1}.

[(FeL^5)$_n$][BF$_4$]$_{2n}$. *Method* (*b*). The complex $[FeL^1_2][BF_4]_2$ (219 mg, 0.25 mmol) and pyromellitic dianhydride (54 mg, 0.25 mmol) were stirred at room temperature in dma (20 cm^3) for 16 h and then heated at reflux for 3 h. The reaction mixture was cooled, an excess of acetyl chloride (5 drops) added and the solution heated at reflux for 1 h. After cooling the reaction mixture was added to an aqueous solution (200 cm^3) containing an excess of NH_4BF_4 to precipitate the polymer and the mixture stirred for 2 h. The solid was filtered off and washed with methanol and acetone repeatedly to remove lower-molecular-weight oligomers. The solid was placed in a flask containing methanol (200 cm^3), heated at reflux for 20 min and then filtered hot. A purple powder was obtained (221 mg, 83%). An analytical sample was obtained by dissolving a sample in dmf and precipitating by dropwise addition to rapidly stirred dichloromethane (Found: C, 54.85; H, 3.70; N, 9.97. Calc. for $C_{52}H_{30}B_2F_8FeN_8O_4\cdot 4H_2O$: C, 55.15; H, 3.36; N, 9.99%). MALDI-TOF mass spectrum: *m*/*z* 1716 ($[FeL^5_2]^+$) and 833 ($[L^5 + 3]^+$). ^{1}H NMR: (CD_3CO_2D) δ 9.32 (br s, 4 H, H$^{3'}$), 9.0–8.2 (m, 10 H, H^3, H^o and H^p), 8.01 (br s, 8 H, H^4 and H^m) and 7.20 (br d, 8 H, H^6 and H^5); [$(CD_3)_2SO$] δ 9.84 (br s, 4 H, H$^{3'}$), 9.16 (br s, 4 H, H^3), 9.0–8.5 (m, 6 H, H^o and H^p), 8.10 (m, 8 H, H^4 and H^m), 7.35 (m, 8 H, H^6 and H^5). IR (Nujol mull): 1775w, 1723s, 1600m, 1515w, 1411w, 1240w, 1050s (br), 866w, 830w, 785m, 750w and 717w cm^{-1}.

Method (*a*). Compound L^5 (150 mg, 0.18 mmol) was suspended in dmf (500 cm^3), $FeCl_2\cdot 4H_2O$ (36 mg, 0.18 mmol) added and the mixture heated at reflux for 18 h. The polymer was isolated as above (98 mg, 51%). This sample gave identical infrared, UV/VIS and ^{1}H NMR spectra to the sample prepared by route (*b*).

[(FeL^6)$_n$][BF$_4$]$_{2n}$. *Method* (*b*). The complex $[FeL^1_2][BF_4]_2$ (212 mg, 0.25 mmol) and terephthaloyl chloride (51 mg, 0.25 mmol) were heated at reflux in dma (20 cm^3) and pyridine (4 cm^3) for 18 h. After cooling the reaction mixture was added to an aqueous solution containing an excess of $[NH_4][BF_4]$ (200 cm^3) to precipitate the polymer and the mixture stirred for 2 h. The solid was filtered off and washed with methanol and acetone repeatedly to remove lower-molecular-weight oligomers. The solid was placed in a flask containing methanol (200 cm^3), refluxed for 20 min and then filtered whilst hot. A purple powder was obtained (150 mg, 60%). An analytical sample was obtained by dissolving the purple powder in warm dmf and precipitating by dropwise addition to rapidly stirred dichloromethane (Found: C, 55.68; H, 4.10; N, 9.66. Calc. for $C_{50}H_{34}B_2F_8FeN_8O_2\cdot 4H_2O$: C, 55.59; H, 3.89; N, 10.38%). MALDI-TOF mass spectrum: *m*/*z* 1613 ($[FeL^6_2 + 1]^+$) and 780 [$(L^6)^+$]. ^{1}H NMR: (CD_3CO_2D) δ 8.31 (br s, 4 H, H$^{3'}$), 8.20 (br s, 8 H, H^3 and H^o) and 7.8–7.2 (m, 20 H, H^p, H^m, H^4, H^6 and H^5); [$(CD_3)_2SO$] δ 10.95 (br s, 2 H, NH), 9.74 (br s, 4 H, H$^{3'}$), 9.13 (br s, 4 H, H^3), 8.75 (m, 4 H, H^o), 8.5–7.9 (m, 12 H, H^p, H^4 and H^m) and 7.30 (m, 8 H, H^6 and H^5). IR (Nujol mull): 3360w (br), 1658m, 1590m, 1510w, 1320w, 1303w, 1240w, 1185w, 1050s (br), 983w, 830w, 784m, 749w and 716m cm^{-1}.

[(FeL^7)$_n$][BF$_4$]$_{2n}$. *Method* (*b*). The complex $[FeL^1_2][BF_4]_2$ (209 mg, 0.25 mmol), adipoyl chloride (50.7 mg, 0.25 mmol) and pyridine (4 cm^3) were heated at reflux in dma (20 cm^3) for 18 h. An excess of acetyl chloride was added and the reaction mixture refluxed for 1 h to end-cap the polymer chains. After cooling the mixture was added to an aqueous solution of NH_4BF_4 (200 cm^3) and stirred for 2 h. The solid was filtered off and washed repeatedly with water, acetone and methanol to remove low-molecular-weight oligomers. The solid was suspended in acetone–methanol (1:1) solution and boiled for 15 min. A purple powder was filtered off (130 mg, 52%). An analytical sample was obtained by dissolving a sample of it in dmf and precipitating by dropwise addition to rapidly stirred dichloromethane (Found: C, 55.04; H, 4.52; N, 10.78. Calc. for $C_{48}H_{38}B_2F_8FeN_8O_2\cdot 3H_2O$: C, 55.33; H, 4.23; N, 10.76%). MALDI-TOF mass spectrum: *m*/*z* 1589 ($[FeL^7_2]^+$) and 767 ($[L^7 + 1]^+$). ^{1}H

NMR: (CD_3CO_2D) δ 8.5–8.0 (m, 16 H, $H^{3'}$, H^3, H^o and H^4), 7.58 (br s, 4 H, H^m), 7.29 (br s, 4 H, H^6), 7.17 (br s, 4 H, H^5), 2.15 (br s, 4 H, CH_2) and 1.39 (br s, 4 H, CH_2); [$(CD_3)_2SO$]: δ 10.48 (br s, 2 H, NH), 9.70 (br s, 4 H, $H^{3'}$), 9.09 (br s, 4 H, H^3), 8.61 (br s, 4 H, H^o), 8.08 (br s, 8 H, H^4 and H^m), 7.23 (m, 4 H, H^5), ≈2.5 (br s, 4 H, CH_2) and 1.84 (br s, 4 H, CH_2). IR (Nujol mull): 3350w (br), 1678m, 1594s, 1520m, 1403w, 1303w, 1240w, 1189w, 1055s (br), 880w, 834m and 787m cm^{-1}.

4′-[*N*-(5-Ethoxy-1,4-benzoquinonyl)-4-anilino]-2,2′:6′,2″-terpyridine (L^9). 1,4-Benzoquinone (0.69 g, 6.27 mmol) dissolved in ethanol (30 cm^3) was added dropwise to L^1 (2.03 g, 6.27 mmol) in ethanol (450 cm^3) at reflux. The reaction mixture was heated at reflux for 18 h. After cooling a small quantity of light green precipitate was filtered from the solution. The filtrate was condensed *in vacuo* to ≈150 cm^3 and the solid filtered off and washed with diethyl ether. Recrystallisation from ethanol afforded a dark red-brown solid (0.97 g, 34%), m.p. 274–278 °C (Found: C, 73.29; H, 4.69; N, 11.84. Calc. for $C_{29}H_{22}N_4O_3$: C, 73.42; H, 4.64; N, 11.81%). EI mass spectrum: *m/z* 474 (M^+), 459 ([$M - CH_3$]$^+$) and 431 ([$M - OEt$]$^+$). ^{1}H NMR [$(CD_3)_2SO$]: δ 9.35 (s, 1 H, NH), 8.79 (d, 2 H, J = 4.9 Hz, H^6), 8.75 (s, 2 H, $H^{3'}$), 8.71 (d, 2 H, J = 7.9, H^3), 8.05 (m, 4 H, H^o and H^4), 7.59 (m, 4 H, H^5 and H^m), 6.11 (s, 1 H, H^Q), 6.03 (s, 1 H, H^Q), 4.11 (q, 2 H, J = 7.0, CH_2) and 1.39 (t, 3 H, J = 6.9 Hz, CH_3). ^{13}C-{^{1}H} NMR [$(CD_3)_2SO$]: δ 183.42, 179.91, 160.39, 155.93, 155.17, 149.57, 148.91, 144.45, 139.58, 137.70, 128.06, 124.77, 123.75, 121.16, 117.85, 115.83, 104.66, 98.78, 65.48 and 13.99. IR (Nujol mull): 3318w, 1660s, 1600m, 1576s, 1532m, 1389m, 1185m, 782s and 722m cm^{-1}.

[CoL^9_2][PF_6]$_2$. The compound L^9 (150 mg, 0.32 mmol) was dissolved in ethanol (700 cm^3) heated at reflux and $CoCl_2 \cdot 6H_2O$ (38 mg, 0.16 mmol) in ethanol (10 cm^3) was added. After 30 min an excess of aqueous ammonium hexafluorophosphate was added and the solution volume reduced to 400 cm^3. The solution was cooled and the resulting solid filtered off and washed with diethyl ether. The solid was then dissolved in acetonitrile and purified by chromatography [silica, acetonitrile–water–saturated KNO_3 (aq) 20:2:1 eluent]. The initial broad maroon band was collected and precipitated by the addition of an excess of aqueous ammonium hexafluorophosphate and recrystallised from acetonitrile–water (1:1) to give a maroon microcrystalline solid (135 mg, 65%) (Found: C, 50.75; H, 3.91; N, 8.02. Calc. for $C_{58}H_{44}CoF_{12}N_8O_6P_2 \cdot 4H_2O$: C, 50.84; H, 3.80; N, 8.18%). ES mass spectrum: 504 (M^{2+}). IR (Nujol mull): 3280w, 1660s, 1585m, 1530m, 1190m and 840s cm^{-1}.

[FeL^9_2][BF_4]$_2$. The compound $Fe(BF_4)_2 \cdot 6H_2O$ (53 mg, 0.16 mmol) in ethanol (15 cm^3) was added to L^9 (150 mg, 0.32 mmol) dissolved in ethanol (700 cm^3) heated at reflux. After 30 min an excess of aqueous ammonium tetrafluoroborate was added and the solution volume reduced to 400 cm^3. The solution was cooled and the resulting solid filtered off and washed with diethyl ether. The solid was then purified by flash chromatography [silica, acetonitrile–water–saturated KNO_3 (aq) 20:2:1 eluent]. The initial purple band was collected and precipitated by the addition of an excess of aqueous ammonium tetrafluoroborate (10 cm^3) and then recrystallisated from aqueous acetonitrile to give a purple microcrystalline solid (95 mg, 50%) (Found: C, 56.51; H, 4.44; N, 8.65. Calc. for $C_{58}H_{44}B_2F_8N_8O_6 \cdot 3H_2O$: C, 56.52; H, 4.06; N, 9.09%). ES mass spectrum: *m/z* 502 (M^{2+}) and 1091 ([$M + BF_4$]$^+$). ^{13}C NMR [$(CD_3)_2CO$]: δ 183.43, 180.03, 160.24, 160.03, 158.09, 152.97, 148.44, 144.18, 140.73, 138.95, 132.05, 128.98, 127.74, 124.18, 123.42, 120.89, 104.77, 99.54, 65.52 and 13.98. IR (Nujol mull): 3270w, 1658m, 1582m, 1525m, 1187m and 1050m (br) cm^{-1}.

[ZnL^9_2][PF_6]$_2$. The compound $Zn(O_2CMe)_2 \cdot 2H_2O$ (39 mg, 0.18 mmol) in ethanol (10 cm^3) was added to L^9 (170 mg, 0.36 mmol) in ethanol (700 cm^3) heated at reflux. After 30 min an excess of aqueous ammonium hexafluorophosphate was added and the solution volume condensed *in vacuo* to 400 cm^3. The solution was cooled and the resulting solid filtered off and washed with diethyl ether. The solid was then dissolved in acetonitrile and purified by flash chromatography [silica, acetonitrile–water–saturated KNO_3 (aq) 20:2:1 eluent]. The initial reddish band was collected and precipitated by the addition of an excess of aqueous ammonium hexafluorophosphate and recrystallised from acetonitrile–water (1:1) to give a red-purple microcrystalline solid (120 mg, 51%) (Found: C, 53.22; H, 3.64; N, 8.55. Calc. for $C_{58}H_{44}F_{12}N_8O_6P_2Zn$: C, 53.40; H, 3.38; N, 8.59%). ES mass spectrum: *m/z* 507 (M^{2+}). ^{13}C NMR [$(CD_3)_2CO$]: δ 183.43, 180.14, 160.25, 154.42, 149.64, 147.93, 144.23, 141.53, 141.27, 131.51, 129.45, 127.89, 123.69, 123.38, 120.83, 104.80, 99.66, 65.57 and 14.01. IR (Nujol mull): 3300w, 1660m, 1640w, 1590s, 1528m, 1239w, 1187m, 1050w, 1020m, 1012m, 1000w, 905w and 838s cm^{-1}.

[Ru(terpy)L^9][PF_6]$_2$. Compound L^9 (200 mg, 0.42 mmol) was dissolved in ethanol (700 cm^3) heated at reflux, [Ru(terpy)Cl_3] (186 mg, 0.40 mmol) in water (50 cm^3) was added and the solution was heated at reflux for 3 h. The solution was filtered through Celite, the solvent removed *in vacuo*, and the residue dissolved in acetonitrile and purified by chromatography [silica, acetonitrile–water–saturated KNO_3 (aq) 20:2:1 eluent]. The initial bright red band was collected and precipitated by the addition of an excess of aqueous ammonium hexafluorophosphate and recrystallised from acetonitrile–water (1:1) to give a red microcrystalline solid (209 mg, 45%) (Found: C, 47.00; H, 3.45; N, 8.53. Calc. for $C_{36}H_{27}F_{12}N_7O_3P_2Ru \cdot H_2O$: C, 47.28; H, 3.13; N, 8.78). ES mass spectrum: *m/z* 404 (M^{2+}) and 954 ([$M + PF_6$]$^+$). ^{13}C-{^{1}H} NMR [$(CD_3)_2CO$]: δ 186.59, 183.52, 160.39, 158.22, 157.97, 155.22, 155.00, 154.73, 152.33, 146.49, 138.28, 136.02, 132.25, 128.86, 127.94, 124.98, 124.72, 124.18, 123.13, 120.98, 119.53, 104.76, 99.26, 65.52 and 14.04. IR (Nujol mull): 3285w, 1665m, 1590s, 1524m, 1240m, 840s and 790m cm^{-1}.

X-Ray crystallography

Crystal data. *For* L^1. $C_{21}H_{16}N_4$, *M* 324.4, monoclinic, space group $P2_1/c$, *a* 9.396(2), *b* 33.792(5), *c* 11.276(2) Å, β 115.129(8)°, *U* 3241(1) Å^3, D_c 1.33 g cm^{-3}, *Z* 8, μ_{Cu} 6.03 cm^{-1}. Crystal size 0.11 × 0.11 × 0.40 mm, $2\theta_{max}$ 140°, minimum and maximum transmission factors 0.83 and 0.94. The number of reflections was 3099 considered observed out of 5673 unique data, with R_{int} 0.018 for 51 pairs of equivalent 0*kl* reflections. After refinement on *F*, final residuals *R*, *R′* were 0.055, 0.077 for the observed data.

For [CuL^1_2][PF_6]$_2$. $C_{42}H_{32}CuF_{12}N_8P_2$, *M* 1002.2, orthorhombic, space group $P2_12_12_1$, *a* 9.124(1), *b* 13.753(2), *c* 33.070(5) Å, *U* 4149.8(9) Å^3, D_c 1.60 g cm^{-3}, *Z* 4, μ_{Cu} 23.43 cm^{-1}. Crystal size 0.09 × 0.13 × 0.30 mm, $2\theta_{max}$ 140°, minimum and maximum transmission factors 0.62 and 0.83. The number of reflections was 3398 considered observed out of 4416 unique data. After refinement on *F*, final residuals *R*, *R′* were 0.052, 0.070 for the observed data.

Structure determinations. Reflection data were measured at 294 K with an Enraf-Nonius CAD-4 diffractometer in θ–2θ scan mode using nickel-filtered copper radiation (λ 1.5418 Å). Data were corrected for absorption using the analytical method of De Meulenaer and Tompa.[31] Reflections with $I > 3\sigma(I)$ were considered observed. The structures were determined by direct phasing and Fourier methods.

For L^1 the structure obtained had the two independent molecules of the asymmetric unit related approximately by a translation of *a*/2, and consequently reflection data with $h = 2n + 1$ were systematically weak. Constrained refinement was used in order to minimise problems caused by the pseudo-symmetry and the relatively small number of observed reflections. Each molecule was modelled as four planar groups, the two outer

pyridyl groups being the same, and with the corresponding groups in each molecule being identical. Three sets of subsidiary coordinates, all with $z = 0$, were used to define the different types of planar groups present, and each group in the two molecules was defined by transformation of the appropriate set of subsidiary coordinates to a local axial system, refineable for rotation and translation. Appropriate x and y coordinates for the subsidiary atoms were refined, and planarity was maintained by keeping $z = 0$ in all cases. Corresponding intergroup distances were slack-constrained to approach equality, but there were no constraints on rotations between groups in the molecules. Hydrogen atoms were included in positions calculated each cycle. Thermal motions were refined using 12-parameter TL rigid-body models for the groups, with the centres of libration of the peripheral groups fixed at their points of attachment to the central ring. The central ring showed no significant librational motion. Hydrogen atom thermal motions were included in the appropriate group.

For $[CuL^1_2][PF_6]_2$, hydrogen atoms were included in calculated positions and assigned thermal parameters equal to those of the atom to which they were bonded. Positional and anisotropic thermal parameters for the non-hydrogen atoms were refined using full-matrix least squares.

For both structures, reflection weights used were $1/\sigma^2(F_o)$, with $\sigma(F_o)$ being derived from $\sigma(I_o) = [\sigma^2(I_o) + (0.04I_o)^2]^{\frac{1}{2}}$. The weighted residual is defined as $R' = (\Sigma w\Delta^2/\Sigma wF_o^2)^{\frac{1}{2}}$. Atomic scattering factors and anomalous dispersion parameters were from ref. 32. Structure solutions were by MULTAN 80[33] and refinements used RAELS for L^1 and BLOCKLS, a local version of ORFLS,[34] for $[CuL^1_2][PF_6]_2$; ORTEP II[20] running on a Macintosh IIcx was used for the structural diagrams, and a DEC Alpha-AXP workstation was used for calculations.

CCDC reference number 186/597.

Acknowledgements

Support from the Australian Research Council is gratefully acknowledged.

References

1 G. Allen and J. C. Bevington (Editors), *Comprehensive Polymer Science: The Synthesis, Characterization, Reactions & Applications of Polymers*, Pergamon, Oxford, 1989; C. J. Feger, M. M. Khojasteh and J. E. McGrath (Editors), *Polyimides: Materials and Chemistry*, Elsevier, Amsterdam, 1989; D. Wilson, H. D. Stenzenberger and P. M. Hergenrother (Editors), *Polyimides*, Blackie & Sons, Glasgow and London, 1990.

2 See, for example, H. Ghassemmi and A. S. Hay, *Macromolecules*, 1994, **27**, 4410; L. R. Dalton, A. W. Harper, R. Ghosn, W. H. Steier, M. Ziari, H. Fetterman,Y. Shi, R. V. Mustacich, A. K.-Y. Jen and K. J. Shea, *Chem. Mater*., 1995, **7**, 1060; H. M. Gajiwala and R. Zand, *Macromolecules*, 1995, **28**, 481; T.-A. Chen, A. K.-Y. Jen and Y. Cai, *J. Am. Chem. Soc*., 1995, **117**, 7295; L. P. Yu, W. K. Chan, Z. H. Peng and A. Gharavi, *Acc. Chem. Res*., 1996, **29**, 13.

3 Z. Bao, Y. Chen and L. Yu, *Macromolecules*, 1994, **27**, 4627; Z. Peng, Z. Bao and L. Yu, *J. Am. Chem. Soc*., 1994, **116**, 6003; Z. Bao, W. K. Chan and L. Yu, *J. Am. Chem. Soc*., 1995, **117**, 12 426.

4 J. E. Mark, H. R. Allcock and R. West, *Inorganic Polymers*, Prentice Hall, Englewood Cliffs, NJ, 1992; C.-T. Chen and K. S. Suslick, *Coord. Chem. Rev*., 1993, **128**, 293; H. R. Allcock, *Adv. Mater*., 1994, **6**, 564; I. Manners, *Angew. Chem., Int. Ed. Engl*., 1996, **35**, 1621.

5 M. Beley and J.-P. Collin, *J. Mol. Catal*., 1993, **79**, 133; G. R. Newkome, F. Cardullo, E. C. Constable, C. N. Moorefield and A. M. W. Cargill Thompson, *J. Chem. Soc., Chem. Commun*., 1993, 925; K. Hanabusa, A. Nakamura, T. Koyama and H. Shirai, *Polym. Int*., 1994, **35**, 231; J. A. Ramos Sende, C. R. Arana, L. Hernández, K. T. Potts, M. Keshavarz-K and H. D. Abruña, *Inorg. Chem*., 1995, **34**, 3348; Y. Liang and R. H. Schmehl, *J. Chem. Soc., Chem. Commun*., 1995, 1007.

6 E. C. Constable, *Adv. Inorg. Chem. Radiochem*., 1986, **30**, 69.

7 R. Hogg and R. G. Wilkins, *J. Chem. Soc*., 1962, 341; P. M. Lutz, G. J. Long and W. A. Baker, *Inorg. Chem*., 1969, **8**, 2529; L. Sacconi, *Pure Appl. Chem*., 1971, **27**, 161; S. Kremer, W. Henke and D. Reinen, *Inorg. Chem*., 1982, **21**, 3013 and refs. therein.

8 R. P. Thummel, V. Hegde and Y. Jahng, *Inorg. Chem*., 1989, **28**, 3264; M. Beley, J.-P. Collin, J.-P. Sauvage, H. Sugihara, F. Heisel and A. Miehé, *J. Chem. Soc., Dalton Trans*., 1991, 3157; C. R. Hecker, A. K. I. Gushurst and D. R. McMillin, *Inorg. Chem*., 1991, **30**, 538; E. Amouyal, M. Mouallem-Bahout and G. Calzaferri, *J. Phys. Chem*., 1991, **95**, 7641; E. Amouyal and M. Mouallem-Bahout, *J. Chem. Soc., Dalton Trans*., 1992, 509; M. Maestri, N. Amaroli, V. Balzani, E. C. Constable and A. M. W. Cargill Thompson, *Inorg. Chem*., 1995, **34**, 2759.

9 W. R. McWhinnie and J. D. Miller, *Adv. Inorg. Chem. Radiochem*., 1969, **12**, 135.

10 E. C. Constable, *Prog. Inorg. Chem*., 1994, **42**, 67; J.-P. Sauvage, J.-P. Collin, J. C. Chambron, S. Guillerez, C. Coudret, V. Balzani, F. Barigelletti, L. De Cola and L. Flamigni, *Chem. Rev*., 1994, **94**, 993; E. C. Constable, in *Transition Metals in Supramolecular Chemistry*, eds. L. Fabbrizzi and A. Poggi, Kluwer, Dordrecht, 1994, p. 81; A. Harriman and J.-P. Sauvage, *Chem. Soc. Rev*., 1996, 41; A. Harriman and R. Ziessel, *Chem. Commun*., 1996, 1707.

11 (*a*) E. C. Constable, A. M. W. Cargill Thompson, P. Harveson, L. Macko and M. Zehnder, *Chem. Eur. J*., 1995, **1**, 360; (*b*) E. C. Constable and P. Harveson, *Chem. Commun*., 1996, 33; (*c*) E. C. Constable and P. Harveson, *Chem. Commun*., 1996, 1821; (*d*) D. Armspach, M. Cattalini, E. C. Constable, C. E. Housecroft and D. Phillips, *Chem. Commun*., 1996, 1823; (*f*) E. C. Constable and R. A. Fallahpour, *J. Chem. Soc., Dalton Trans.*, 1996, 2389; (*e*) B. Whittle, S. R. Batten, J. C. Jeffery, L. H. Rees and M. D. Ward, *J. Chem. Soc., Dalton Trans*., 1996, 4249.

12 E. C. Constable and A. M. W. Cargill Thompson, *J. Chem. Soc., Dalton Trans*., 1992, 3467; 1995, 1615.

13 M. P. O'Niel, M. P. Niemczyk, W. A. Svec, D. Gosztola, G. L. Gains III and M. R. Wasielewski, *Science*, 1992, **257**, 63; M. Ohkohchi, A. Takahashi, N. Mataga, T. Okada, A. Osuka, H. Yamada and K. Maruyama, *J. Am. Chem. Soc*., 1993, **115**, 12 137; A. Osuka, S. Nakajima, T. Okada, S. Taniguchi, K. Nozaki, T. Ohno, I. Yamazaki, Y. Nishimura and N. Mataga, *Angew. Chem., Int. Ed. Engl*., 1996, **35**, 92; C. A. Hunter and R. K. Hyde, *Angew. Chem., Int. Ed. Engl*., 1996, **35**, 1936; M. P. Debreczeny, W. A. Svec and M. R. Wasielewski, *Science*, 1996, **274**, 584.

14 G. M. Bower and L. W. Frost, *J. Polym. Sci., Part A*, 1963, **1**, 3135; F. Higashi, S.-I. Ogata and Y. Aoki, *J. Polym. Chem. Ed*., 1982, **20**, 2081; H. M. Gajiwala and R. Zand, *Macromolecules*, 1993, **26**, 5976.

15 G. D. Storrier and S. B. Colbran, *J. Chem. Soc., Dalton Trans*., 1996, 2185.

16 W. Spahni and G. Calzaferri, *Helv. Chim. Acta*, 1984, **67**, 450.

17 E. Campaigne, W. E. Budd and G. F. Schaefer, *Org. Synth*., 1963, **Coll. Vol. II**, 225.

18 E. P. Platnova, L. I. Polishchuk, Ya. I. Kurys′ and V. D. Pokhodenko, *Elektrokhimiya*, 1990, **26**, 326; K. Kaleem, F. Chertok and S. Erhan, *Prog. Org. Coat*., 1987, **15**, 63; K. Kaleem, F. Chertok and S. Erhan, *J. Polym. Sci., Part A, Polym. Chem*., 1989, **27**, 865.

19 M. Z. Barakat, S. K. Shebab and M. M. El-Sadr, *J. Chem. Soc*., 1958, 901.

20 C. K. Johnson, ORTEP II, Report ORNL-5138, Oak Ridge National Laboratory, Oak Ridge, TN, 1976.

21 E. C. Constable, J. Lewis, M. C. Liptrot and P. R. Raithby, *Inorg. Chim. Acta*, 1990, **178**, 47.

22 G. D. Storrier, Ph.D. Thesis, University of New South Wales, 1996.

23 C. D. Craver and T. Provder (Editors), *Polymer Characterisation: Physical Properties, Spectroscopic, and Chromatographic Methods*, American Chemical Society, Washington, DC, 1990.

24 R. Allmann, W. Henke and D. Reinen, *Inorg. Chem*., 1978, **17**, 378.

25 D. F. Evans, *J. Chem. Soc*., 1959, 2003.

26 E. C. Constable, A. M. W. Cargill Thompson, D. A. Tocher and M. A. M. Daniels, *New J. Chem*., 1992, **16**, 855.

27 T. Ohsaka, Y. Ohnuki, N. Oyama, G. Katagiri and K. Kamisako, *J. Electroanal. Chem. Interfacial Electrochem*., 1984, **161**, 399.

28 J. M. Rao, D. J. Macero and M. C. Hughes, *Inorg. Chim. Acta*, 1980, **41**, 221.

29 G. R. Newkome, R. Güther, C. N. Moorefield, F. Cardullo, L. Echegoyen, E. Perez-Cordero and H. Luftmann, *Angew. Chem., Int. Ed. Engl*., 1995, **34**, 2023; H. F. Chow, I. Y.-K. Chan, D. T. W. Chan and R. W. M. Kwok, *Chem. Eur. J*., 1996, **2**, 1085.

30 IGORPRO 2.0™, WaveMetrics Inc., Lake Oswego, OR, 1995.

31 J. De Meulenaer and H. Tompa, *Acta Crystallogr*., 1965, **19**, 1014.

32 J. A. Ibers and W. C. Hamilton (Editors), *International Tables for X-Ray Crystallography*, Kynoch Press, Birmingham, 1974, vol. 4.

33 P. Main, MULTAN 80, University of York, 1980.

34 W. R. Busing, K. O. Martin and H. A. Levy, ORFLS, Oak Ridge National Laboratory, TN, 1962.

Received 23*rd April* 1997; *Paper* 7/02778H